

Measurement of the spatial distribution of the spectral response variation in the field of view of the ASD spectrometer input optics

Martin P. Lévesque, Stéphane Giroux, Jean-Pierre Ardouin

DRDC - Valcartier Research Centre

Defence Research and Development Canada

Scientific Report

DRDC-RDDC-2014-R122

December 2014

Measurement of the spatial distribution of the spectral response variation in the field of view of the ASD spectrometer input optics

Martin P. Lévesque, Stéphane Giroux, Jean-Pierre Ardouin

DRDC - Valcartier Research Centre

Defence Research and Development Canada

Scientific Report

DRDC-RDDC-2014-R122

December 2014

Abstract

A new goniometer is under development. It will be used for the measurement of the spectro-polarimetric BRDF (Bidirectional Reflectance Distribution function). For practical reasons, the selected spectrometer is an ASD field spectro-radiometer. Its optical head is built with an optical fibre cable bundle that makes it easy to use. Only the optical head has to be mounted on the goniometer, the main body of the spectrometer remains aside. The ASD spectrometer has several input optics (bare fibres, lenses and telescopes) and several tests were conducted to determine which one is the best for the goniometer. The conclusion: none of them. By construction, the ASD spectrometer does not have a homogeneous field of view (FOV). The optical fibre bundle does not uniformly sample the FOV. This can be partly solved by defocusing the optics. But, all the tested optics suffers from severe spectral dispersion or other artefacts. However, a simple optical design based on the use of an off-axis mirror can do the job. This will be used for the optical reading head of the goniometer.

Significance to defence and security

This study aims to improve the hyperspectral detection capability. To do this, a better knowledge about the reflectance of material present into the scene is required. The optical signature acquisitions of the surface are done with spectrometers, which can generate measurement artefacts. The non-uniformity of the field of view (FOV) of the instrument is one of the sources of error that this study reveals. Moreover, this report proposes solutions to remediate this issue.

Résumé

Un nouveau goniomètre est en développement. Il sera utilisé pour les mesures de BRDF (fonction de distribution de réflectance bidirectionnelle) spectrales et polarimétriques. Pour des raisons pratiques, le spectromètre sélectionné est le spectro-radiomètre portable de la compagnie ASD. Sa tête optique est faite avec un câble de fibres optiques qui la rend facile à utiliser. Seulement la tête optique doit être montée sur le goniomètre, le corps principal du spectromètre reste à côté. Le spectromètre ASD a plusieurs optiques d'entrées (fibres nues, lentilles et télescopes) et plusieurs tests ont été faits pour déterminer lequel est le meilleur pour le goniomètre. La conclusion : aucun d'entre eux. De par sa construction, le spectromètre ASD n'a pas un champ de vue homogène. Le faisceau de fibres optiques n'échantillonne pas uniformément le champ de vue. Ceci peut être résolu en mettant l'optique hors foyer. Mais, toutes les optiques testées souffrent de dispersion spectrale sévère et de d'autres artéfacts. Cependant, un design optique simple basé sur l'utilisation d'un miroir hors-axe peut faire l'affaire. Celui-ci sera utilisé pour faire la tête de lecture du goniomètre.

Importance pour la défense et la sécurité

Cette étude vise à améliorer la capacité de détection hyperspectrale. Pour ce faire, une meilleure connaissance de la réflectance des matériaux présent dans la scène est requise. L'acquisition des signatures optiques des surfaces se font au moyen de spectromètres, lesquels peuvent générer des artéfacts de mesures. La non-uniformité du champ de vue (FOV) de l'instrument est une des sources d'erreur que cette étude révèle. De plus, ce rapport propose des solutions afin d'y remédier.

Table of contents

Abstract	i
Significance to defence and security	i
Résumé	ii
Importance pour la défense et la sécurité	ii
Table of contents	iii
List of figures	iv
List of tables	vi
1 Introduction.....	1
2 Spectral and polarimetric reflection coefficients	3
2.1 Definition of a polarimetric and spectral reflection coefficient.....	3
2.2 Goniometer under development	4
3 Characteristics of the inspected optics	6
4 Setup and methodology for the measurement of the spectrometer FOV	9
5 Measurement of the bare fibre bundle of the ASD-6175 spectrometer	12
6 Measurement of the 8 deg. FOV lens of the ASD-6175 spectrometer.....	14
7 Measurement of the 1 deg. FOV lens of the ASD-6175 spectrometer.....	19
8 Measurement of the 1 deg. FOV telescope of the ASD-6175 spectrometer	22
9 Measurement of the FOV of an off-axis mirror	25
10 Measurement of the FOV of a tilted 50 mm f/4 spherical mirror.....	28
11 Tests done with the scrambler device	30
12 Conclusion	32
References	34
Annex A Band selection	35
Annex B Measurement of the ASD-6175 8 degrees FOV lens used with the ASD-6175 spectrometer	37
B.1 Sensor scintillation	41
Annex C Measurement of the 1 degree FOV lens used with the ASD-6175 spectrometer	42
Annex D Measurement of the 1 degree FOV telescope used with the ASD-6175 spectrometer	44
Annex E Measurement of the two 8 degrees FOV lens (ASD-6175 and ASD-16132 lens) with the ASD-16132 spectrometer.....	47
Annex F Measurement of the FOV of the 50 mm f/4 tilted spherical mirror.....	50
List of symbols/abbreviations/acronyms/initialisms	53

List of figures

Figure 1: Polarized and spectral bidirectional reflectance angles.	3
Figure 2: Scheme of the goniometer under design. The expected distance between the optic and the sample is about 0.5 m.	4
Figure 3: Scheme of the optical fibre bundle and lens coupling.	6
Figure 4: Calculation of the position of the image plane with the geometric optics.	7
Figure 5: Estimation of the FOV.	8
Figure 6: Equipment setup: ASD spectrometer, optical fibre bundle, 1 deg. and 8 deg. lenses, 1 deg. telescope, scanning mechanism and light source.	9
Figure 7: Blackbody light source.	10
Figure 8: Scanning mechanism.	10
Figure 9: Scanned FOV showing the distribution of the fibres for the different detectors of the spectrometer ASD-6175 and creation of a composite RGB image. This was measured with the 8 deg. FOV lens.	11
Figure 10: Image scanned with the bare fibre.	12
Figure 11: Profiles of the scanned image of Fig. 10 for 3 different wavelengths, each one corresponding to a different waveband detector.	13
Figure 12: Geometry of the measurement setup and measured FOV for the bare fibre.	13
Figure 13: Measurement of the 8 deg. lens with different focus adjustments, for an object distance $O = 287$ mm ($f + O = 298$ mm in Table 2).	15
Figure 14: Comparison of the FOV of the 8 deg. lens for two different spectrometers	15
Figure 15: Multiple acquisitions with rotation of the FOV for the defocus 8 deg. lens.	16
Figure 16: Summation of 4 rotated measurements (0, 90°, 180 ° and 270°) with various defocuses of the 8 deg. lens.	16
Figure 17: A: Profile extraction and averaging, B: evaluation of the profile radius at half height and C: encircle energy for the measured radius for two different defocuses.	17
Figure 18: Total count of the encircle energy in relation with the defocus adjustment.	18
Figure 19: Measured FOV for the 8 deg. lens.	18
Figure 20: Refocused ($df = i = 12.7$ mm) and out of focus ($df = 0$, i.e., focus for a very far object) images with the 1 deg. lens for a close object at 762 mm from the lens.	19
Figure 21: Geometry of the measurement setup for the 1 deg. lens (with $df = 12.7$ mm). While the three bands are equally present in the middle of the FOV, the outer ring is dominated by short wavelength.	20
Figure 22: Effect of the FOV of the bare fibre located at the focal point of the entrance optics on the resulting footprint.	21
Figure 23: focused and out of focused images produced with the 1 deg. FOV telescope.	22
Figure 24: Blind spot produced by the obscuration caused by the secondary mirror.	22
Figure 25: Effect of the limited FOV of the optical fibre placed in the detector pupil.	24

Figure 26: Measurement of the FOV of an off-axis mirror restricted to the 42deg. off-axis zone.....	25
Figure 27: Scans of various defocused images for an object at a distance (O+f) of 955 mm from the off-axis mirror.	26
Figure 28: Effect of the partial illumination of the optical-fibre bundle head.....	27
Figure 29: Optical design based on a tilted 50 mm spherical f/4 mirror; the input FOV is 0.5 degree.....	28
Figure 30: Setup with the tilt f/4 50 mm spherical mirror mounted on the scanner.	29
Figure 31: Scans of various defocused images for an object at a distance (O+f) of 1.3m from the tilted spherical mirror 50 mm f/4.	29
Figure 32: Scrambler device place at the entrance of the optical fibre bundle.....	30
Figure 33: Evaluation of the scrambler effect with the 50 mm tilted f/4 spherical mirror.	30
Figure 34: Evaluation of the scrambler effect with the ASD 1 and 8 degrees lenses.....	31

List of tables

Table 1: List of tested optics.	7
Table 2: Theoretical position of the image plane, for various object positions.	8
Table 3: Estimated FOV of the different lenses, for a fibre bundle diameter $h=1.7$ mm at the focal point.	8
Table 4: Calculated foot print and blind spot dimensions in relation with the object distance.	23
Table A1: Spectral bands associated with each detector	35
Table A2: Selected bands	35
Table A3: Scanned images for some specific bands	36
Table B1 to B7: Measurement of the FOV of the 8 deg. lens, lens-to-source distance: O+f=298 mm, ...	
Table B1: ... focus adjustment: $df=0$ mm	37
Table B2: ... focus adjustment: $df=1.27$ mm	37
Table B3: ... focus adjustment: $df=2.5$ mm	38
Table B4: ... focus adjustment: $df=3.81$ mm	38
Table B5: ... focus adjustment: $df=5.08$ mm	39
Table B6: ... focus adjustment: $df=6.35$ mm	39
Table B7: ... focus adjustment: $df=7.52$ mm	39
Table B8: FOV comparison for two focus adjustments and for different object distances.	40
Table B9: Measure of the sensor scintillation (noise).	41
Table C1 to C5: Measurement of the FOV of the 1 deg. lens, ...	
Table C1: ... lens-to-source distance: O+f=43 mm, focus adjustment: $df=0$ mm	42
Table C2: ... lens-to-source distance: O+f=381 mm, focus adjustment: $df=0$ mm	42
Table C3: ... lens-to-source distance: O+f=762 mm, focus adjustment: $df=0$ mm	43
Table C4: ... lens-to-source distance: O+f=762 mm, focus adjustment: $df=12.7$ mm	43
Table C5: ... lens-to-source distance: O+f=956 mm, focus adjustment: $df=12.7$ mm	43
Table D1: Measurement of the FOV of the 1 deg. telescope, lens-to-source distance: 43 mm, focus adjustment: $df=0$ mm (supposedly focus to the infinite).	44
Table D2: Measurement of the FOV of the 1 deg. telescope: acquisitions for various distances of the object plane.	45
Table D3: Measurement of the FOV of the 1 deg. telescope: acquisitions for various focus adjustments.	46
Table E1 to E5: Measurement of the FOV of the (s/n 16132) 8 deg. lens with the field spectrometer ASD s/n 16132...	
Table E1: ... focus adjustment: $df=0$ mm.	47
Table E2: ... focus adjustment: $df=1.27$ mm.	48
Table E3: ... focus adjustment: $df=5.08$ mm.	48
Table E4: ... focus adjustment: $df=6.35$ mm.	49
Table E5: ... focus adjustment: $df=7.62$ mm.	49

Table F1 to F6: Measurement of the FOV of the tilted 50 mm f/4 spherical mirror with the field spectrometer ASD s/n 16132. Distance to object plane: $O+f=1500$ mm, ...	
Table F1: ... focus adjustment: $df=0$ mm (focus to the infinite).....	50
Table F2: ... focus adjustment: $df=10$ mm.	50
Table F3: ... focus adjustment: $df=20$ mm.	51
Table F4: ... focus adjustment: $df=40$ mm. (image plane)	51
Table F5: ... focus adjustment: $df=50$ mm.	51
Table F6: ... focus adjustment: $df=60$ mm	52

1 Introduction

For surveillance applications, it is important to have accurate knowledge of the scenes of interest. This knowledge is acquired by measuring the scene, analysing it and by characterising its components. A good scene analysis requires also a-priori knowledge. First, the illumination needs to be known as well as the atmospheric transmission between the scene and the sensor for the transformation of the image content from at-sensor radiance to surface reflectance. Finally, a database of known material reflectance (or spectral library) is required to identify the presence of these materials in the scene. A good understanding of the phenomenology facilitates the interpretation of the observations.

A single “global” spectral reflection coefficient is often not sufficient for a good characterisation of a material. There is variability in the spectrum which depends on other parameters. Materials are absorbers, reflectors and diffusers. Furthermore, materials may have highly variable surfaces finishes which alter their optical properties. This issue is partially solved by the independent measurements of the spectral and Bidirectional Reflectance Distribution Function (BRDF). The BRDF is the measurement of the reflection coefficient for different combinations of illumination and observation angles. However, with the increasing refinement of the sensing equipment, the traditional BRDF needs to be upgraded to meet the new requirements. To fully exploit sensor data, polarimetric and spectral BRDF is required (“spectro-polarimetric BRDF” as mentioned in Ref. 1).

However, there exists no extensive public database that describes the reflectivity of various materials in relation with the spectral wavelength and polarization angle simultaneously. Only separated and uncorrelated measurements exist. Therefore, most of the common material will have to be measured again with a goniometric sensor that takes into account all these parameters simultaneously. Such a polarimetric and spectral sensor is not common (Ref. 1). Most of the recent goniometers measure only spectral BRDF (Refs. 2, 3) and, to our knowledge, they have not considered potential issues that can occur when measuring textured objects. Many of those goniometers, operating in the 0.4 to 2.5 microns region, are built around an Analytical Spectral Device (ASD) spectrometer, which is known to have an inhomogeneous field of view and this may cause problems when measuring textured objects. The only reported tentative to characterise the ASD field of view are published in Refs. 4 and 5, and these studies were not made specifically for the development of a goniometer system.

A spectral and polarimetric goniometer will have to be equipped with a small spectral sensor, which will be associated with a filter wheels that will contain several polarisers. A polariser filter wheel will probably also be mounted on the light source. This will allow measuring the 1) capability of the material to polarise the incident light and 2) its capability to depolarise an incident polarised light beam.

The conception of such a goniometer presents several difficulties. First, it is difficult to find polarisers and quarter wave plates (for circular polarisation) with a large transmission waveband. They will seriously affect the spectral measurement. This difficulty can be resolved by using several polarisers (for the same polariser angle) made of different materials. This would allow covering the spectrometer waveband, one small band at a time. The second difficulty is the dimension of the goniometer components. These components will have to be mounted on

articulated arms. Thus, their weights and volumes are factors that limit the goniometer design. The light source can be of moderate size and does not present a big challenge. The filter wheels add other constraints to the design but the difficulty is still manageable. The real issue is the spectrometer. A spectrometer is usually a large package containing a complex optical design. Very small spectrometers exist, but the known ones do not have the desired/appropriate waveband width. Some spectrometers (Ref. 6 and 7) which operate in the desired waveband (0.3 to 2,5 μ m, and eventually 0.3 to 12 μ m), are relatively small, but still too big for the considered design.

Among the possible spectrometer candidates, there is the ASD spectro-radiometer (Ref. 6). The particularity of this device is that its optical input is an optical fibre bundle. This allows decoupling the reading head from the spectrometer package. Hence, only the small reading head could be mounted on the goniometer arm. Physically, this presents an attractive solution to the issue of weight and volume. It remains to see if the optical properties are appropriate.

This study examines the spatial distribution of field of view (FOV) of the optical input of the ASD. The optical fibre bundle makes the device very easy to use, but it may hide some side effects. This is the subject covered by this report.

Here is how this report is structured. Before beginning the FOV analysis, this report begins by describing briefly the desired goniometer in Chapter 2. This explains why the ASD spectrometer is a good fit for this project. Chapter 3 explains how the reading head is coupled to the spectrometer with an optical fiber bundle and raises some concern about this design. It also lists the available ASD lens (with their characteristics) than can be mounted on this optical fibre bundle and modifies its FOV. The measurements of these FOVs are done with the experimental setup and methodology shown in Chapter 4.

Chapters 5 to 11 report the measurements and evaluations done on different optical devices. Chapter 5 characterises the ASD spectrometer when it is used with the bare fiber, while Chapters 6 to 8 reports the evaluations of the 8 deg. FOV lens, 1 deg. FOV lens and 1 deg. FOV telescope, respectively. Because none of these optics were satisfying, homemade optics (made with an off-axis f/2 parabolic mirror and a tilted f/4 spherical mirror) were also tested and reported in Chapters 9 and 10. This tilted f/4 mirror produced the best results and it is the source of inspiration for the optical design selected for the goniometer. Finally, Chapter 11 presents the result of the use of the ASD scrambler device, which is supposed to improve the uniformity of the FOV, but does not meet the expectation.

Annexes A to F contain the tables showing the results of the FOV scans for all optical devices in various conditions. Hence, the sceptic reader has the possibility to see them and verify the conclusions presented in the previous chapters.

This work was performed between August 2010 and September 2011, first under the 15dd HYperspectral iMage EXploitation (HYMEX) TDP and ended under the 10cd25 COTS VNIR/SWIR HSI Sensor project.

2 Spectral and polarimetric reflection coefficients

2.1 Definition of a polarimetric and spectral reflection coefficient

The reflection coefficient is the intensity ratio between the reflected light beam and the incident light beam. But this does not consider how the energy is distributed in space. The reflection can be Lambertian (diffuse) or specular with a combination of back and forward scattering. The general case could be represented by the following model:

$$\text{Reflection coefficient: } \rho(\alpha_i, \varepsilon_i, p_i, \alpha_r, \varepsilon_r, p_r, \lambda), \quad (1)$$

where α_i and ε_i are the azimuth and elevation angles and p_i is the polarization matrix of the incident light beam, α_r , ε_r and p_r are for the reflected light beam, and λ the observed wavelength (Fig. 1). One may note that the azimuth angles α_i and α_r can be coupled into a single variable ($\alpha_r - \alpha_i$), but this may not be adequate for some surface finish like brushed aluminum which presents grooves aligned in a specific direction. The polarisation matrix includes the circular and linear polarisation (angle directions and ratios).

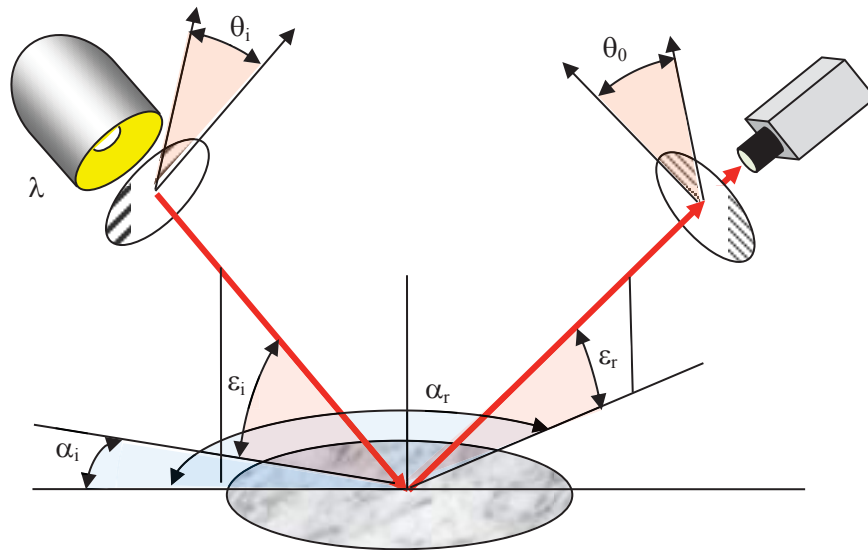


Figure 1: Polarized and spectral bidirectional reflectance angles.

Presently, such reflection coefficient knowledge is, most of the time, limited to a combination of the independent reflection angles $\rho(\alpha_i, \varepsilon_i, \alpha_r, \varepsilon_r)$ and spectral $\rho(\lambda)$ coefficients. For most diffusing surfaces, this is good enough. But for glossy surfaces, particularly for surfaces with coating causing interferential effect, the spectral coefficient cannot be dissociated from the observation angles (Ref. 8). Therefore, we have to build our own goniometer, do measurements and build our new polarimetric and spectral BRDF database. For classical spectral BRDF,

i.e., without considering the polarisation effects, theory and instrumentation are well described in Refs. 1, 2 and 9.

2.2 Goniometer under development

The desired goniometer design is similar to the one presented in Ref. 1. However, the goniometer we wish to build will be of smaller dimension; the arc circle will be between 1m and 2m of diameter. It will be used for the analysis of relatively small material samples. Figure 2 illustrates such a goniometer where the light source and spectrometer are mounted on semi-circular rings, which allows their displacement in azimuth and elevation angles. The analysed sample will be placed in the middle of goniometer on a robotic (rotating) table. Once in a while, the robotic sample support will replace the sample by a Spectralon plate for calibration needs. Possibly, the sample will be rotated to average the texture of the sample during the acquisition. But this will not be necessary if the FOV is spectrally uniform.

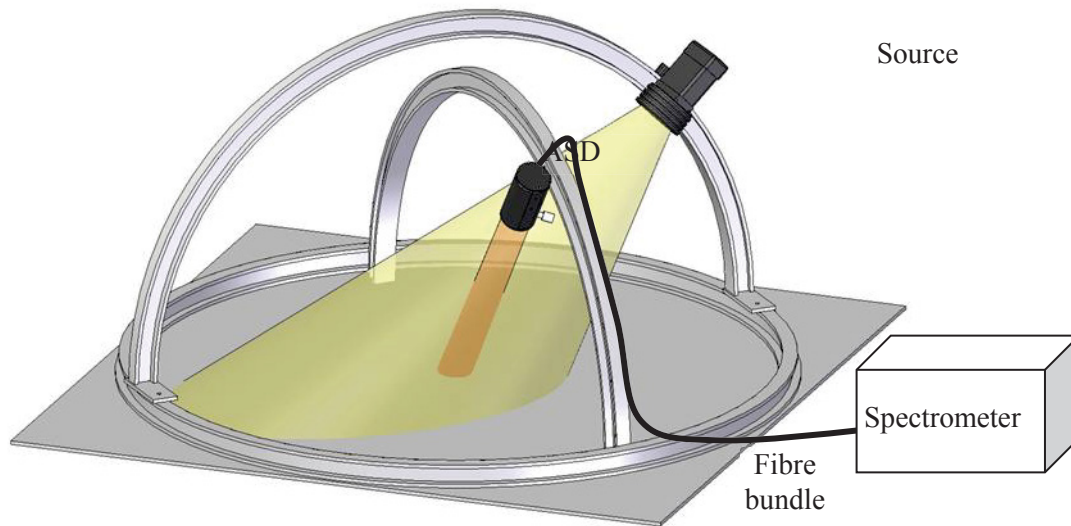


Figure 2: Scheme of the goniometer under design. The expected distance between the optic and the sample is about 0.5 m.

Another potential alternative design is the one published in Ref. 10. Rather than moving the sensor, this is the sample surface that is tilted at various angles. This considerably simplifies the goniometer design. However, this approach is discarded because it is expected that liquids and wet materials will be measured, which obviously cannot be tilted.

For practical reasons, it is planned to build the small goniometer with an ASD spectrometer as the sensor. First, this spectrometer is already in our possession, which considerably reduces the cost of the project. Second, this spectrometer is a piece of equipment that will not be permanently attached to the goniometer setup and can thus be used for other application. Third, and the most important reason, only the spectrometer reading head will be mounted on the goniometer, which reduces the size and weight on the goniometer arms and makes the manipulation easier. The ASD spectrometer reading head is composed of an optical fibre bundle, which collects the light and bring this light to the spectrometer device, which remains beside the goniometer (Fig. 2). This

goniometer configuration offers an appreciable advantage in term of weight and manipulation capabilities. However, it was brought to our attention that this configuration has also an undesirable secondary effect. Mac Arthur and al. (Ref. 4 and 5) indicate that the field of view (FOV) of the ASD spectrometer is not homogenous, i.e., the radiometric sensitivity and spectral response vary inside the FOV.

It is expected that the goniometer will be used for the measurement of heterogeneous materials such as vegetation and complex manmade objects. It is important that the measured spectra do not suffer from variations caused by the match (or miss-match) between the material texture and the FOV sensitivity variations. Therefore, the spectrometer FOV must be measured and characterized. The most important point that must be verified is the homogeneity of its spectral response.

3 Characteristics of the inspected optics

The ASD spectrometer uses an optical fibre bundle that redirects the input light toward the spectrometer gratings. This simplifies the use of the spectrometer. This spectrometer is in fact three different spectrometers in one. The visible and near infrared (VNIR) spectrometer uses silicon linear array from 350 to approximately 1000 nm. The first short wave infrared spectrometer (SWIR1) uses an InGaAs photodiode detector covering the 1000 to 1800 nm waveband and, the second short wave infrared spectrometer (SWIR2) also uses an InGaAs photodiode covering the 1800 to 2500 nm waveband. The three spectrometers share the same optical input. The input light beam is split by separating the optical fibre into three distinct bundles (Fig. 3). But the inconvenience is that each detector does not see exactly the same scene elements as the other. This is not an inconvenience for objects with homogeneous surfaces, but this can create major spectral differences for objects made of several heterogeneous materials.

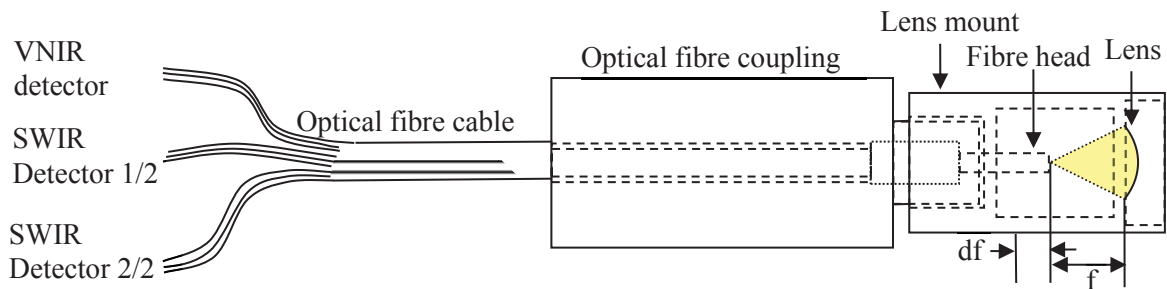


Figure 3: Scheme of the optical fibre bundle and lens coupling.

The optical fibre bundle can be used bare or with different input optics which produces different FOV. They are listed in Table 1. At this time, we have not selected the input optic that will be best for the goniometer, so all of them will be analysed. The real FOV and the spatial and spectral FOV uniformity will be measured for different distances of the source object and with different defocus positions “ df ” (defined in Fig. 4).

These lenses are used for the measurement of objects at distances of about 0.5m or more. The default position of the optical fibre head (i.e., where it is mounted, see Fig. 3), is the focal point of the lens for a focus to the infinite. However, it is possible to move back the optical fibre head inside the bundle coupling and refocus the image when the measurement is done on an object at close range. This is the “ df ” value shown in Figs. 3 and 4, i.e., the variation of the focus position. Mechanically, the optical-fibre coupling device allows us to retract the optical fibre by 12 mm. Above this point, the optical-fibre bundle becomes too slack and may fall from the coupling device.

The common sense in optics tells us that the optics must be well focused to obtain the best signal. However, the next chapters will show that a well-focused image is not good in this case. With a well-focused image, each optical fibre sees a different scene element. This is not good if the scene is textured because the measured spectrum depends on the match between the spectrometer FOV pattern and the scene texture. Therefore, a defocused image better serves this cause than a well-focused image because the FOV of the individual fibre is increased (blur) and all fibre FOV

overlap each other. This makes the global FOV more uniform. The questions are; where are the focus images (for the different optics) and how defocused should the optic be?

Table 1: List of tested optics.

Optics Parameter	Bare fibre	8 degrees FOV lens	1 degree FOV lens	1 degree FOV Newtonian telescope
FOV (degrees) (company specification)	25	8	1	1
D: Input optical diameter (mm)	1.7	8.4	50	49.3
focal length (mm) (estimated from lens dimensions)	--	10.6 (estimated from lens dimensions)	104 (estimated from lens dimensions)	107 (estimated from telescope dimensions)
focal length (mm) (deduced from measured optical properties)		11.41		90 (see annex D)
f/number focal length / diameter		f/1.4	f/2	f/2

Theoretically, the position of the focused image plane “i” can be estimated with the design of the optical lens and position of the imaged source. Considering the geometric optics (Fig. 4), the position ‘of the well-focused image plane is calculated with the relation “ $i/f=f/O$ ”, where “f” is the focal length, “i” the distance of the image plane from the focal point and “O” the distance of the imaged object. Table 2 indicates the positions of the image planes for the inspected optics. It takes into account only short object distances because the listed distances are similar to those considered for the designed goniometer.

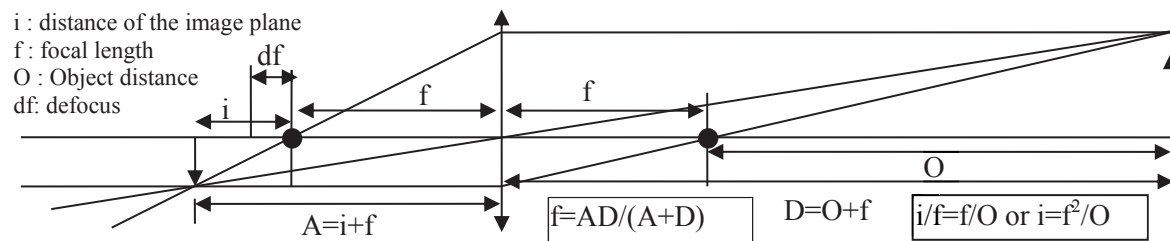


Figure 4: Calculation of the position of the image plane with the geometric optics

The lens FOV can also be estimated with the optics geometry. Basically, the FOV is calculated by projecting the disk area of the fibre bundle through the lens. When the end of the fibre bundle is placed at the focal plane, this generates a flat wave front output which is represented by parallel propagating rays (red, black or cyan rays in Fig. 5). Table 3 provides the FOVs calculated using the measured physical dimension of the lenses and optical-fibre bundle. The estimations almost match the FOV declared by the company.

These are the theoretical estimations. In the next chapters, we validate them with experimental measurements.

Table 2: Theoretical position of the image plane, for various object positions.

	1 def FOV lens (f=104 mm)		1deg FOV telescope (f= 107 mm)		8 deg FOV lens (f= 10.6 mm)	
Object to lens (f+O) distance (mm)	O (mm)	i (mm)	O (mm)	i (mm)	O (mm)	i (mm)
43	Case of virtual image	---			32.4	3.5
298					287.4	3.9
381	277	39				
473	369	29.3			462.4	0.24
762	658	16.5				
955*	851	12.7*				
1241**			1134	10.1*		
Focus range: The head of the fibre bundle can be pull back by 12 mm approximately. *: Minimal object distance for a focused image at the maximum focus capability of the 1 deg. lens. **: Minimal object distance for a focused image at the maximum focus capability of the 1 deg. telescope.						

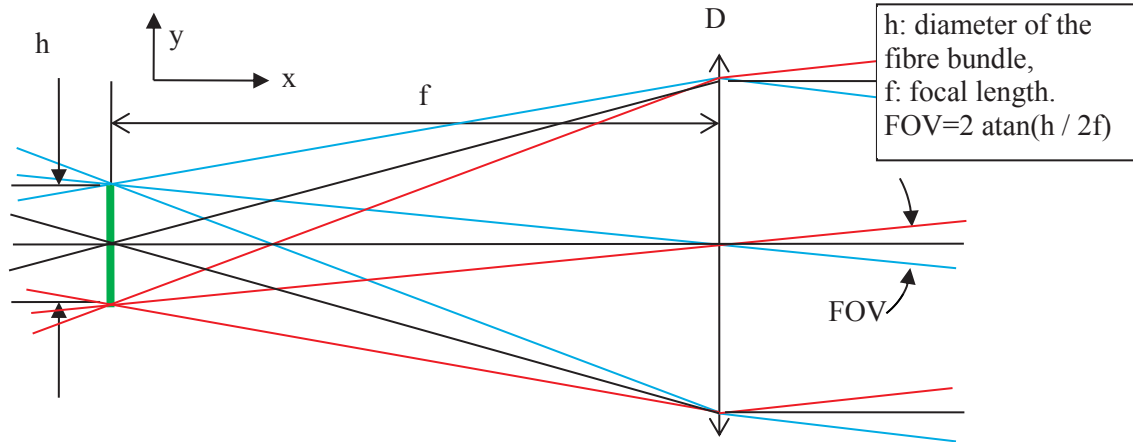


Figure 5: Estimation of the FOV

Table 3: Estimated FOV of the different lenses, for a fibre bundle diameter $h= 1.7$ mm at the focal point.

	1 deg. lens	1 deg. telescope	8 deg. lens
f	104	107	10.6
$FOV=2 \operatorname{atan}(h/2f)$	0.94 deg.	0.94 deg	6.9 deg.

4 Setup and methodology for the measurement of the spectrometer FOV

The theoretical FOV estimations contain approximations; the diffraction is not considered in geometrical projection, the focal length measurements are inaccurate and each optical fibre has its own limited FOV. Therefore, the real FOV must be measured and characterized. The inspection of the quality of the goniometer optical input is mandatory. This will be a laboratory instrument that will acquire measurement of reference for comparison and calibration of future field measurements and it is necessary that these laboratory measurements are done accurately. The FOV of the optical input must be well known and exempt of artefacts, or at least with known and controlled artefacts.

The experimental setup is illustrated in Figs. 6, 7 and 8. The experiment consists of measuring the spectra of one point source which is displaced to several locations in the examined FOV. By displacing correctly the optical-fibre bundle or the light source (this is a reversible system), all the measurements can be used to form a single hyper spectral image.

The light source (Fig. 7) consists of an integrating sphere with a pin hole of 1.6 mm ($1/16^{\text{th}}$ inches). At the distance used in the experimental setup, the pin hole is smaller than the resolution of one optical fibre FOV (when well-focused).

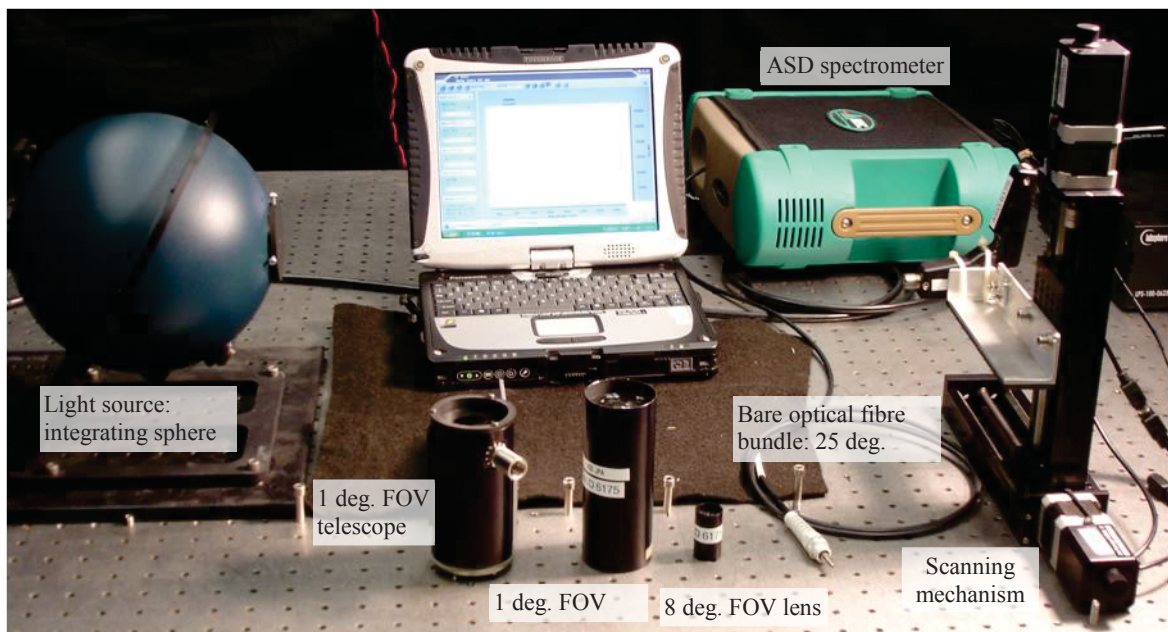


Figure 6: Equipment setup: ASD spectrometer, optical fibre bundle, 1 deg. and 8 deg. lenses, 1 deg. telescope, scanning mechanism and light source.

The spectrometer input optic, is mounted on a scanning mechanism (Fig. 8) that moves over a two dimensional grid. At each grid position, one spectrometer measurement is taken of the point source. This scanning pattern generates an image of the spectrometer field of view as a function

of the wavelength. Typically, an area of 6x6 cm is scanned with a resolution of 2.4 mm, producing an image of 25x25 pixels. These are the dimensions of most of the images presented in this document but, when needed, the same area can be scanned at a higher resolution.

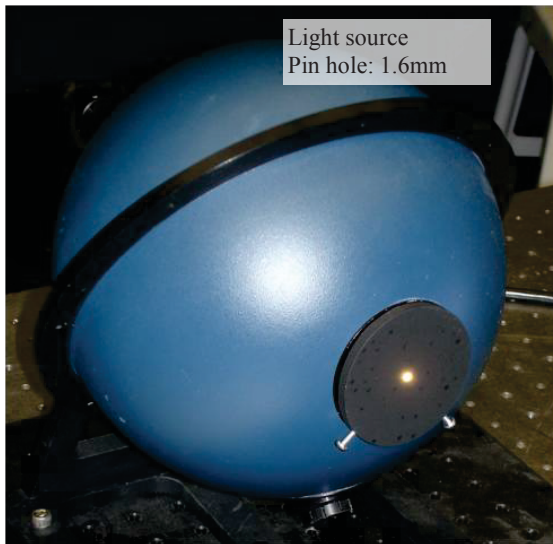


Figure 7: Light source.

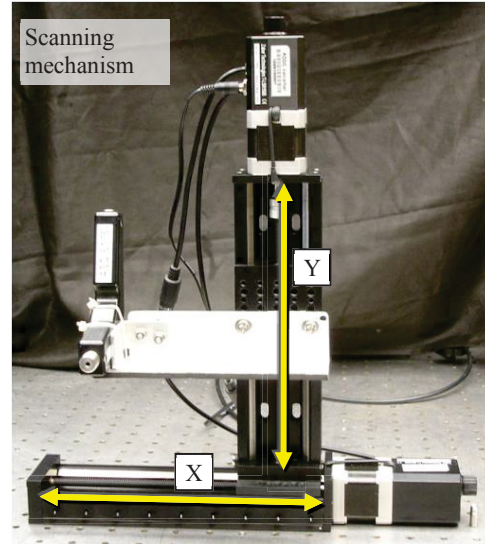


Figure 8: Scanning mechanism.

The resulting spectral image format is “BIP”, i.e., “Band Interleave by Pixel”. In this format, all pixel bands are contiguous. The “BIP” encoding is (band, sample, line), i.e.,: (band 1, band 2, ... band n of pixel 1), (...of pixel 2) ..., etc. This format is useful for spectrum analysis, but not for image analysis. Therefore, the image format is converted to “BSQ”, i.e., Band Sequential: (sample, line, band), or: image (band1), image (band2), etc.

For the analysis of the spectrometer FOV, all the spectral bands are not required. The variations of the spectral sensitivity in the FOV are principally caused by the random splitting of the optical fibres into three separate groups. All image bands from the same detector have the same FOV distribution (more or less a certain blur cause by the spectral dispersion of the lens). Only one spectral band from each spectrometer detector is necessary for the analysis of the uniformity of the optical input FOV. The index of the selected image band numbers are 325, 1015 and 1720. They are shown in Fig. 9. Annex A explains why these band numbers are chosen. When these images are used as RGB image components, they produce a single color image which shows the spectral non-uniformity of the ASD FOV. Fig. 9 shows without any doubt that the ASD’s FOV is not uniform. This measurement was done with the 8 deg. lens. Other measurements are shown in Annexes B to F for the other ASD lenses and other tested optical elements.

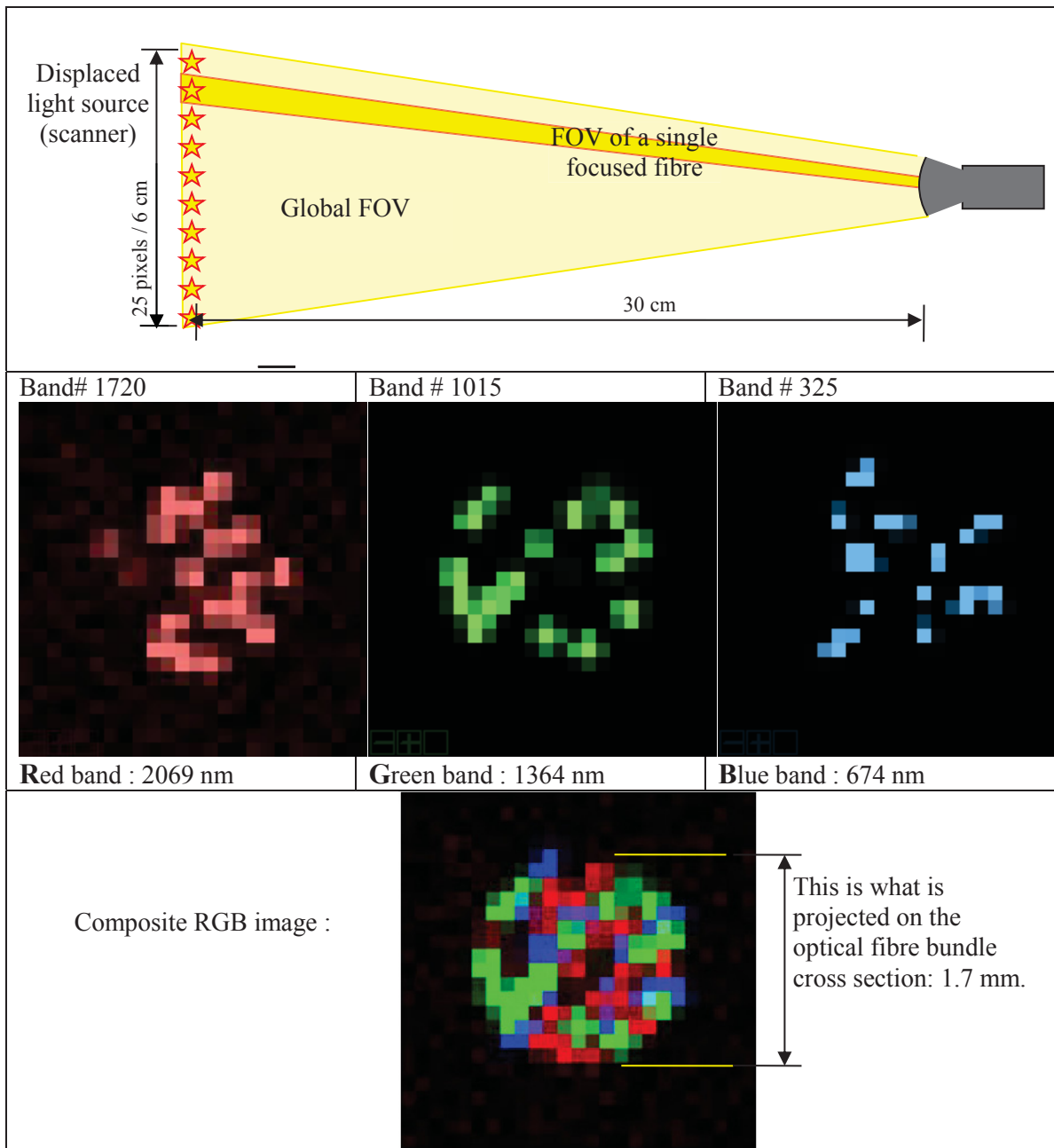


Figure 9: Scanned FOV showing the distribution of the fibres for the different detectors of the spectrometer ASD-6175 and creation of a composite RGB image. This was measured with the 8 deg. FOV lens.

5 Measurement of the bare fibre bundle of the ASD-6175 spectrometer

Presumably, the bare optical fibre should have a FOV of 25 degrees (company specification). The optical fibre FOV was measured on the test bench. The light source was at a distance of 106 mm. The fibre head scanned area of 60x60mm with a step of 0.6mm, producing the 100x100 pixels image of Fig. 10. For the other figures (Fig. 13 and the following), the low resolution scans are 25x25 pixels, i.e., the pixel size is 2.4 mm.

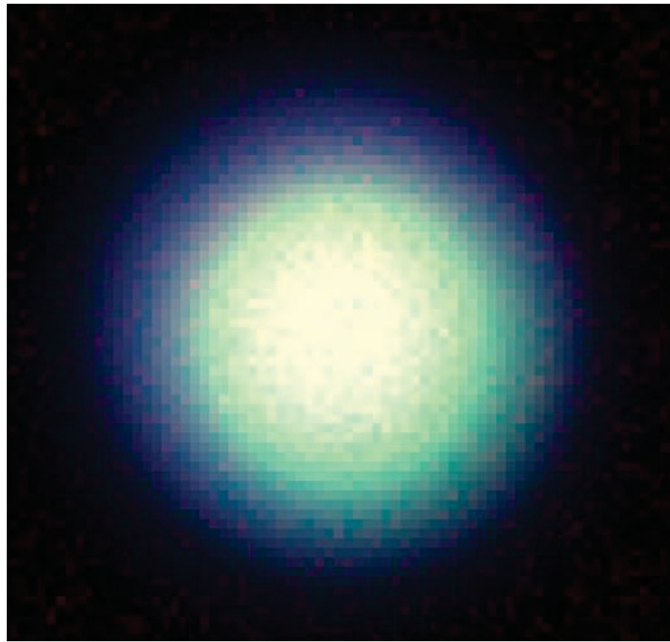


Figure10: Image scanned with the bare fibre.

One may notes the bluish halo around the central white spot. Figure 11 shows the profiles for each one of the 3 selected spectral bands. Not surprisingly, the bare fibre has a FOV which depends on the wavelength. Figure 12 illustrates the scene geometry. At a wavelength of 1364 nm, the measured FOV is 12 degrees at half height of the intensity profile. This is very far from the expected 25 degrees. In fact, the 25 degrees is for the full profile width, from zero to zero sensitivity, but this is not the appropriate way of defining a FOV. The 12 degrees corresponds to the efficient FOV, which empirically represents around 80% of the total FOV sensitivity.

In conclusion, 1) the bare fibre FOV is smaller than expected and 2) the FOV does not have a uniform spectral sensitivity. The spectrometer response is higher at shorter wavelength in the periphery of the FOV. The measured FOV is too large for a goniometer application where an angular resolution of 1 to 5 degrees is desired. However, the central spot is quite uniform. An iris could be used to limit the FOV to the central part of bare-fibre FOV and the spectral response

would be acceptable. However, the optical-fibre bundle has a very small input aperture and this makes the spectrometer not very sensitive. This would also make a very slow goniometer (long exposure time) and the analysis of a single surface could take days. It is almost mandatory to use an input optic to increase the size of the aperture of the collecting area.

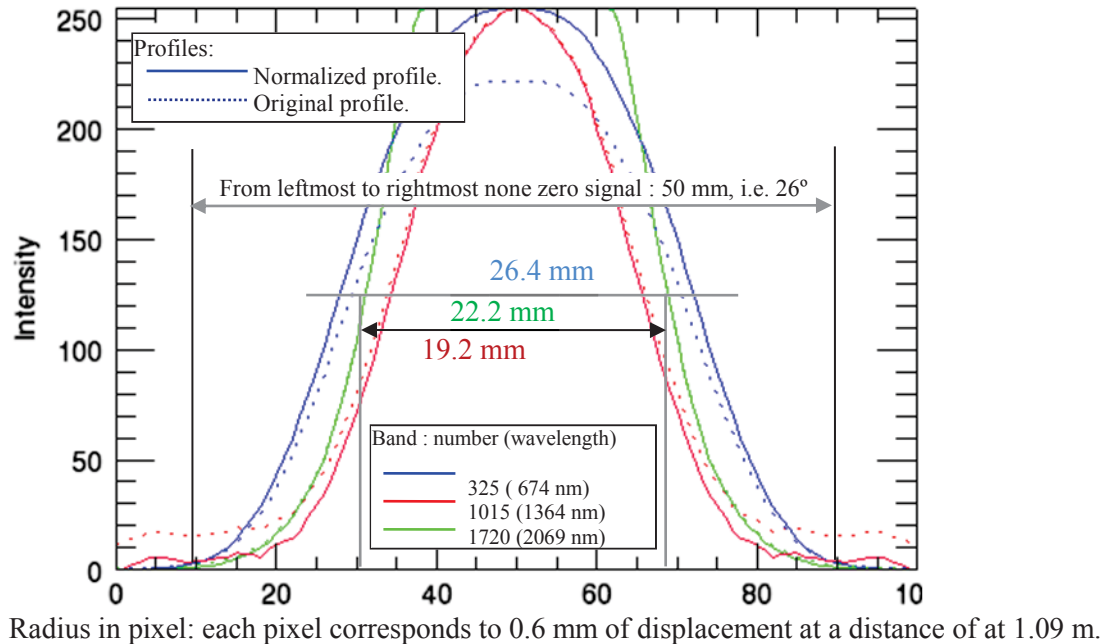


Figure 11: Profiles of the scanned image of Fig. 10 for 3 different wavelengths, each one corresponding to a different waveband detector.

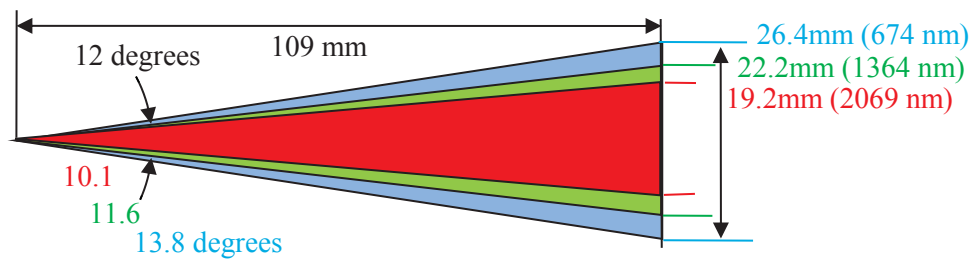


Figure 12: Geometry of the measurement setup and measured FOV for the bare fibre.

6 Measurement of the 8 deg. FOV lens of the ASD-6175 spectrometer

Figure 9 was acquired with the 8 deg. FOV lens. This shows that, when the lens is well focused, the spectrometer FOV is very not uniform. Each optical-fibre sees a different part of the FOV. Figure 13 is produced with this same optic, but with different focus adjustments. The exact focus position, i.e., the image plane, (for the close light source at 1m) was found at $df=1.27$ mm (see Fig. 4), rather than the calculated focus offset of 3.2 mm. This position, along with the distance of the images object, allows the calculation of the exact focal length, which is 11.41mm (Table 1). This also indicates to us that the optical-fibre bundle had never been placed (intentionally or not) at the focal plane of the lens. As described previously, common sense in optics tells us to place the sensor at the focal plane of the input optic but, in this case, it is preferable not to do that.

The spectral uniformity of the FOV is increased by blurring (defocusing) the image. The defocus is done by moving back the optical-fibre bundle inside the fibre coupling device. The FOVs, of the individual optical fibre, increase and they finally overlap each other. Ideally, the FOV of a single fibre should be equal to the entire FOV, but it was not possible to reach such a focus offset without decoupling the fibre bundle. The maximum offset allowed by the mechanical system is 12.7 mm.

Figure 13 indicates clearly that the blurring (by defocussing) improves the spectral uniformity in the FOV. However, in the RGB distribution of the fibres, the final blurred image indicates that the fibres are not well distributed. There is a predominant green (1354 nm) on the left side and a predominant red (2069 nm) on the right side. The optical fibres (in the bundle) are randomly separated into three groups of fibres and then coupled to each of the three spectrometers detectors. If each one of the fibres was identified and systematically separated and regrouped with an RGB-RGB pattern, the global FOV would be more uniform, even with a smaller defocus.

In order to remove the doubt about the effect of the optical-fibre bundle, the measurements were done using the same scanning mechanism, the same 8 def. FOV lens, but with two different ASD spectrometers of the same conception, in other words, with a different optical-fibre bundle. The results are presented in Fig. 14. Obviously, the measurements are similar, excepted that the RGB distributions of the fibres in the bundle are different. Hence, if the two spectrometers would have to measure the same textured object, they would produce different measurements.

In Fig. 13, the 8 deg. lens has almost the desired FOV uniformity when it reaches the maximum defocus. However, the green left side and red right side of the FOV are still too apparent. By averaging the measurements via the rotation of the inspected object, or the rotation of the spectrometer reading head, it is possible to complete the "FOV smoothing process". How much defocus or how many rotations are required? The following figures answer this question. Figure 15 shows the combination of one, two and four rotated measurements. With four rotations, the color predominance completely disappears. Even with the rotation averaging, Figure 16 indicates that a high defocus is still desirable. Also, this method is efficient at the condition that the images are well aligned, i.e., center of the FOV in the center of the image, which is not obvious with the scanner. Before doing a summation, the images must be re-centered on the pixel of maximum

intensity or on the geometric center of intensity of the pixel distribution. In Figs. 15 and 16, the image rotations were simulated with a software rotation operator.

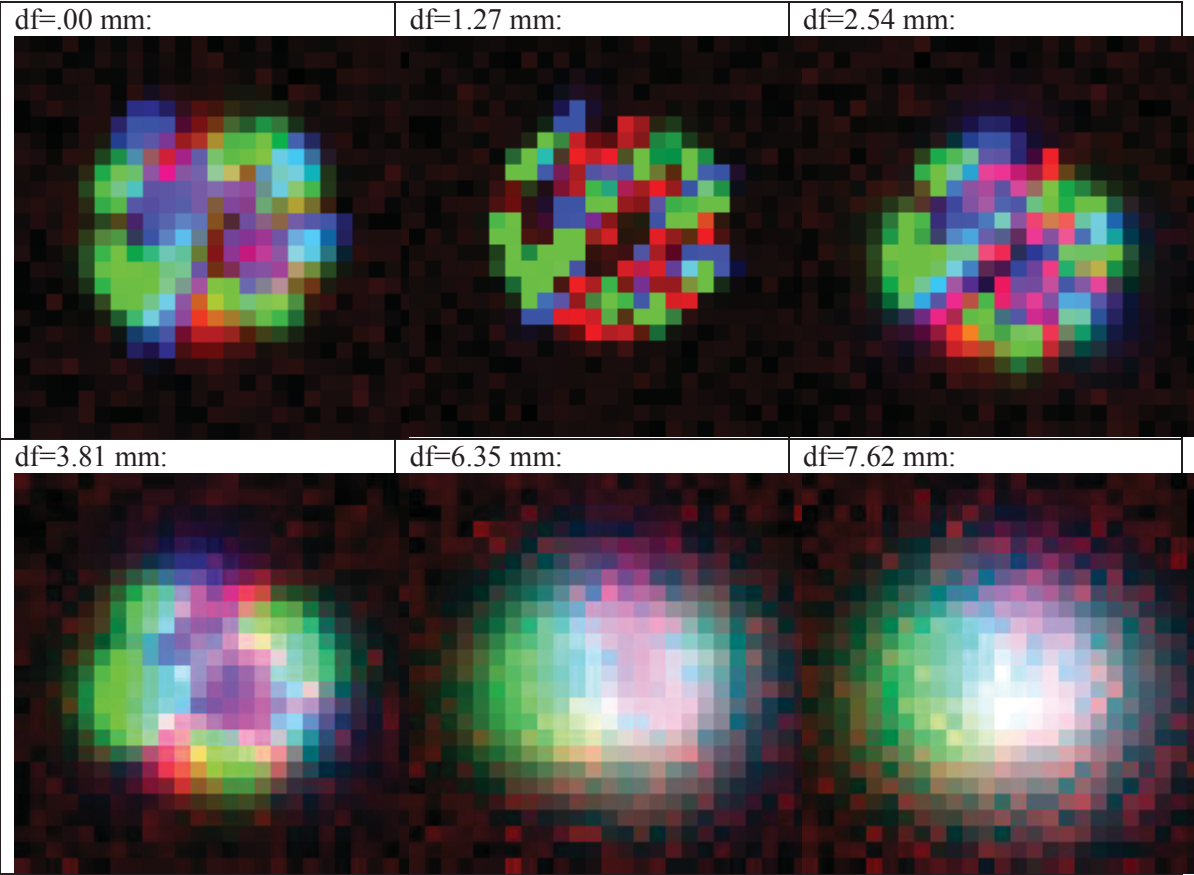


Figure 13: Measurement of the 8 deg. lens with different focus offset adjustments (df), for an object distance $O=287\text{ mm}$ ($f+O=298\text{ mm}$ in Table 2) ($R=2069\text{ nm}$, $G=1364\text{ nm}$ and $B=647\text{ nm}$).

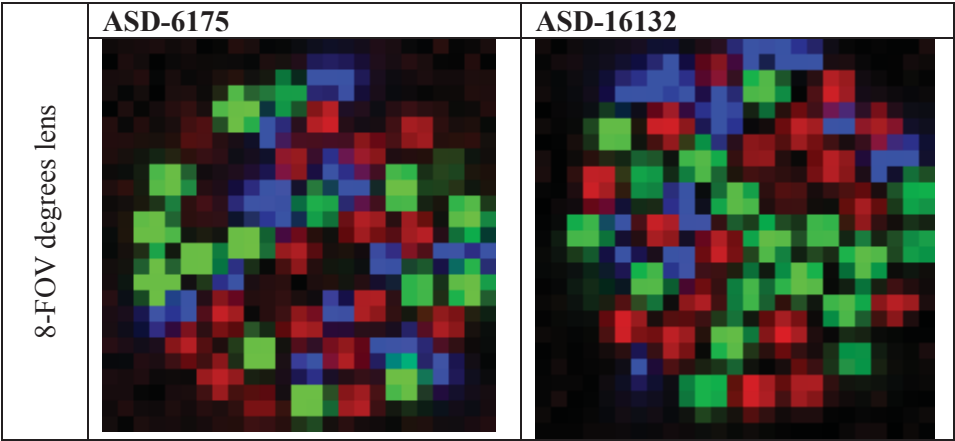


Figure 14: Comparison of the FOV of the 8 deg. lens for two different spectrometers.

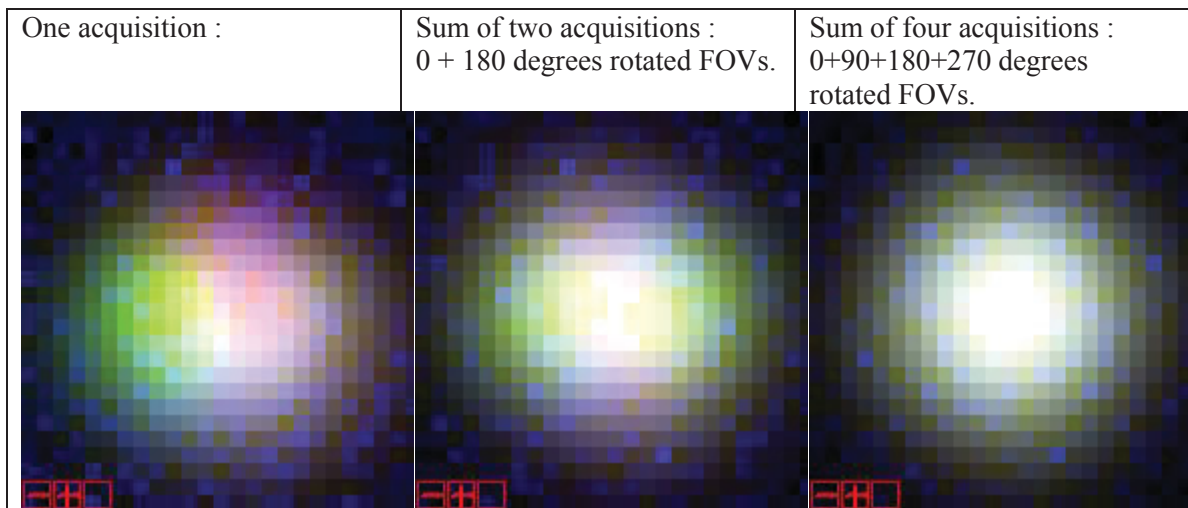


Figure 15: Multiple acquisitions with rotation of the FOV for the defocus 8 deg. lens.

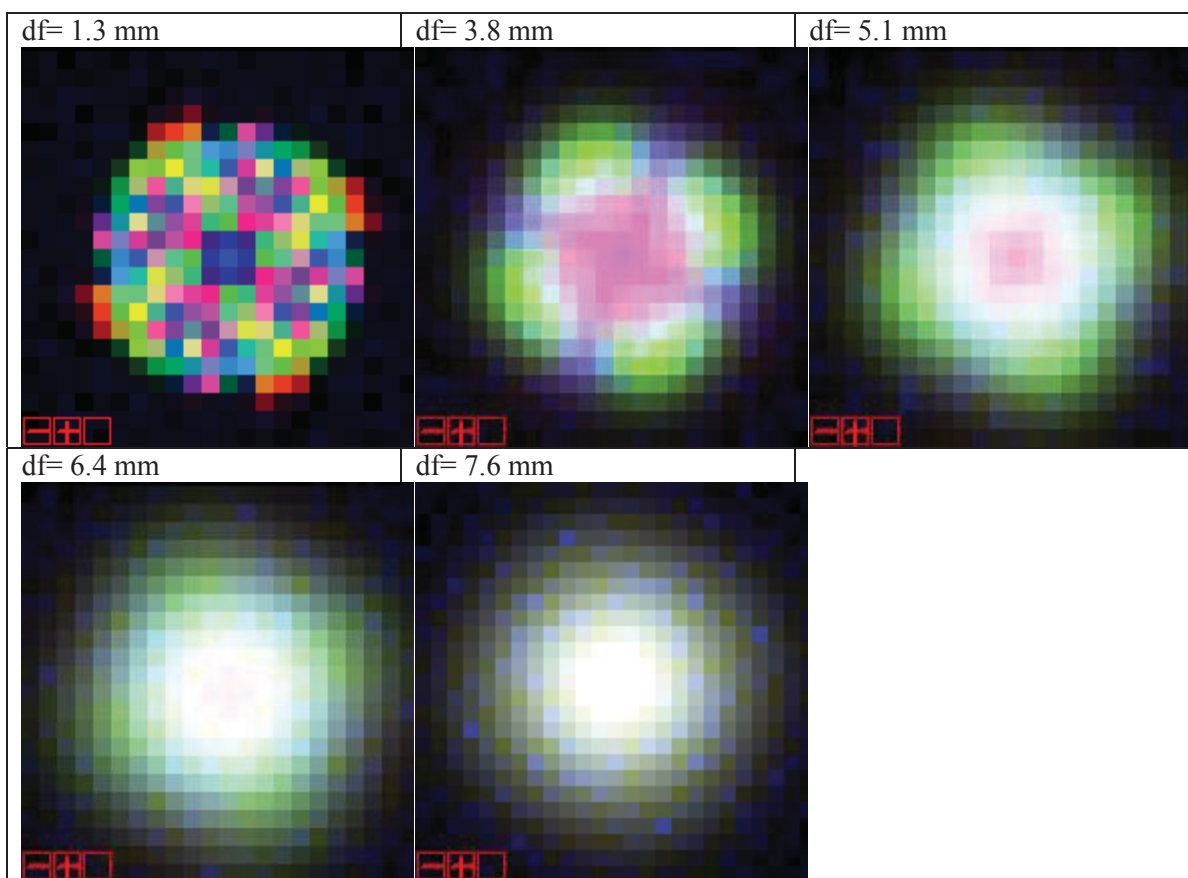


Figure 16: Summation of 4 rotated measurements (0, 90°, 180 ° and 270°) with various focus offsets of the 8 deg. lens.

For an acquisition done with a future goniometer, the FOV rotation could be done with an optical rotator but 1) this adds several mirrors on the optical path and 2) this is not good for polarimetric measurements. A simpler technique consists in placing the measured sample on a turn table and by acquiring several measurement of the rotating object.

More detailed measurements and profiles are shown in Annex B for the 8 degrees lens. The images are useful for the visual perception of the FOV, but the extracted profiles are more practical for the measurement of the width of the FOV at half-height. A single profile is very erratic because it depends on the match between the extracted profile and the alignment of the optical fibres. So, the presented profiles are the result of the averaging of several profiles acquired at different angles.

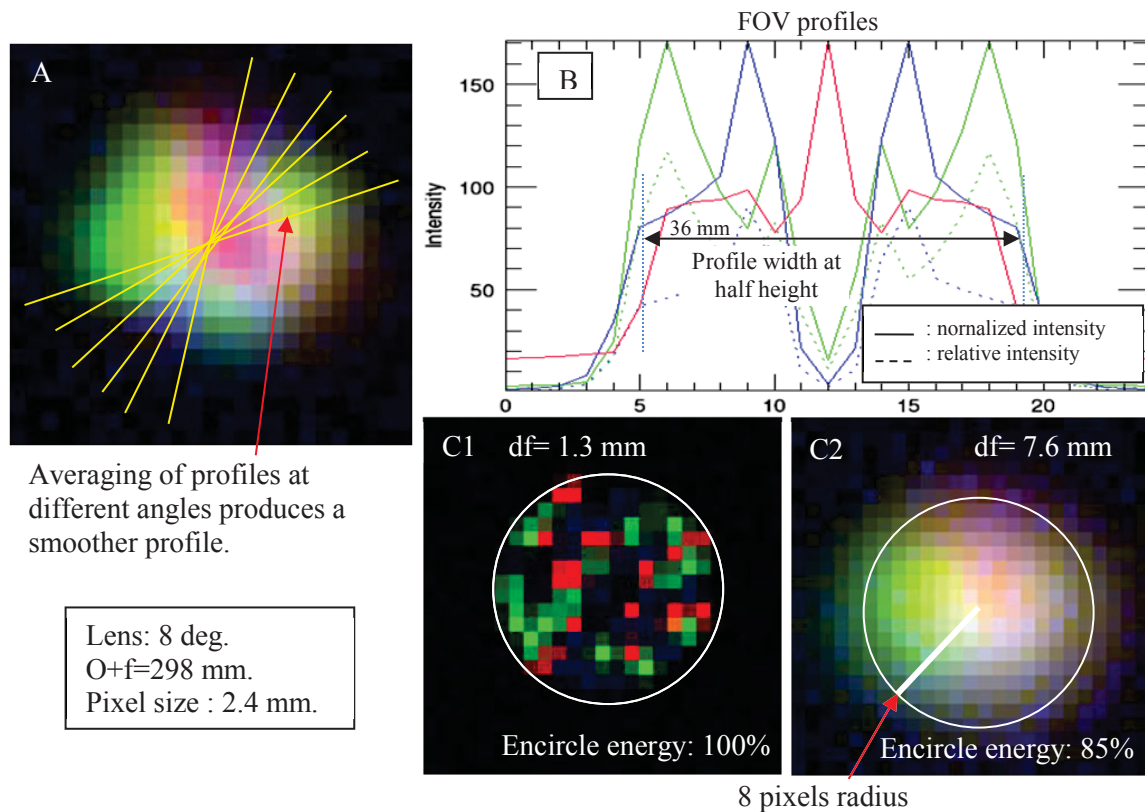


Figure 17: A: Profile extraction and averaging, B: evaluation of the profile radius at half height and C: encircle energy for the measured radius for two different focus offsets.

In Figure 17, the encircled pixels correspond to the FOV width defined by the profile cut at half height. By defocusing the image, the profiles enlarge, but the width at half height is almost constant, at least for the range of defocus that was analysed. However, this means that a certain amount of energy becomes spread in a peripheral halo which could be cut-off by an optical stop field. However, Fig. 18 shows that even with the strongest defocus, the encircle energy (total count) remains above 85% of the initial focused FOV, which is very acceptable. Note that the individual fibers have larger FOV but the global FOV of the entire optical fiber bundle remains almost the same. The aim is making the FOV of each optical fiber matching the bundle FOV.

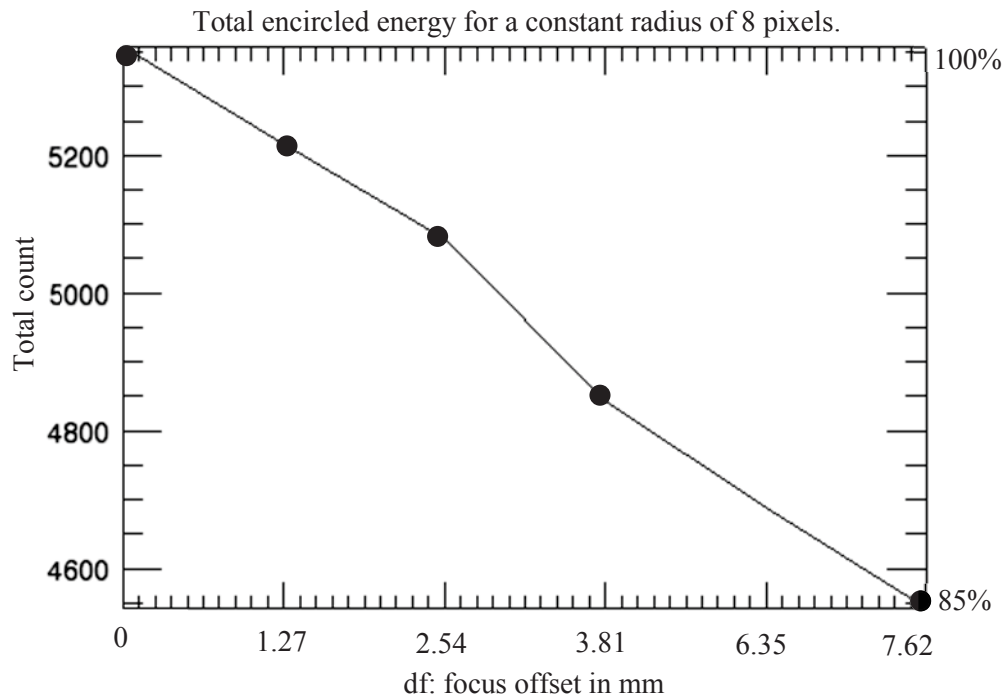


Figure 18: Total count of the encircle energy in relation with the defocus adjustment.

The FOV, specified by the ASD Company, for this optics is 8 degrees (Table 3). The real lens FOV is evaluated with the size and distance of the observed object (scanning light). The width at half height of the profile in the Table B2, for a well-focused image, is 36 mm. This is for an object distance (O+f) equal to 298 mm. With these values, the effective FOV is 6.9 degrees (Fig. 19).

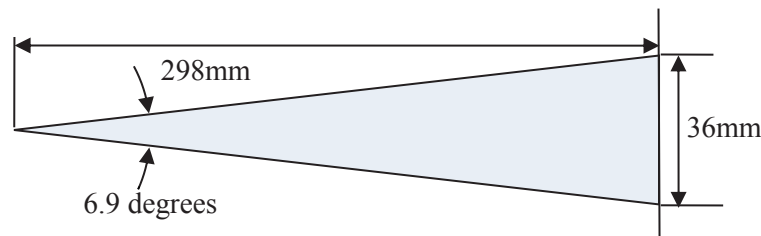


Figure 19: Measured FOV for the 8 deg. lens.

In summary, the 8 deg. lens is a good candidate for the goniometer optic on the condition that 1) it is used out of focus, 2) the measured object is rotated at least four times and 3) the required angular resolution of the BRDF is not better than 8 to 10 degrees. For BRDF measurement requiring a higher angular resolution, it is not adequate.

7 Measurement of the 1 deg. FOV lens of the ASD-6175 spectrometer

The 1 degree FOV lens was also measured. The details of the measurements are presented in Annex C. These measurements, particularly the profiles presented in Annex C, show the effect of the dispersion of the refraction index of the glass used to make the lens. Obviously, this optic is not an optimized achromatic lens, but a single chromatic lens (which minimizes the effects of the spectral transmission through the material). Therefore, the focus image presents a bluish halo around a central white spot while the defocused image presents a reddish halo.

The default position for the head of the optical fibre bundle is at the focal point of the lens, i.e., at $df=0$. Then the optical system is focused for an object located at an infinite distance. With this setting, only the parallel input beams are focused on the optical fibre. The sensed footprint (Fig. 20B) should be the geometric projection of the input lens (50 mm of diameter) plus the 1 degree of divergence (FOV). The minimum object distance where it is possible to focus on an image is 1 m. This corresponds to the maximum possible focus offset adjustment of $df=12.7$ mm (Fig. 20A).

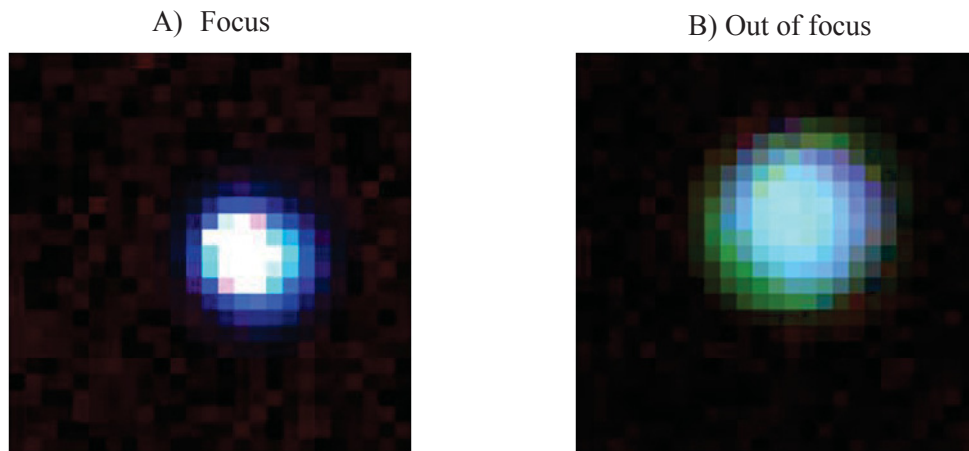


Figure 20: Refocused (image plane at $df=12.7$ mm) and out of focus ($df=0$, i.e., focus for a very far object) images with the 1 deg. lens for a close object at 762 mm from the lens.

Several FOV image profiles are shown in Annex C. Fig. 21 presents the FOV geometry for the case where the image is focused ($df=12.7$ mm). For the short wavelengths (detector 1; 300 to 970 nm) the FOV is 1.3 degrees while for the long wavelengths (detector 3; 1761 to 2500 nm) the FOV is only 0.65 degrees. The FOV varies with the object distance and focus adjustment. The effect that is responsible for this wavelength dependent FOV is the lens chromaticity. In summary, this lens may be a source of trouble for a goniometer input optic.

The measurement of the footprint of this lens indicates another potential problem. The footprint is smaller than expected. When the optical fibre head is placed at the focal point of the lens, i.e., for

a focus done for an infinite distance, the spectrometer captures only the incoming parallel beam plus the 1 degree of divergence. Hence, the footprint should be approximately 50 mm of diameter (the lens diameter). But, it is only 22 mm. This is explained as follow: this optical design is based on an optical fibre that has a FOV around 25 degrees. 25 degrees is the FOV where the fibre can sense a signal, without considering the peripheral attenuation. So, an $f/2$ 50 mm lens should match the bare fibre FOV. However, Chapter 5 indicated that 80% of the sensed signal is inside a FOV of 12 degrees. Outside this 12-degrees FOV, the signal is severely attenuated. Introducing this 12-degrees FOV inside the optical design, Fig. 22 shows that we get this observed 22 mm profile width. The periphery of the 50 mm lens is useless, a 25 mm $f/4$ lens would have done the same job. This also limits the real footprint on the object plane. Now, considering the bare fibre FOV profile into the optical design, the measured footprint illustrated in the drawings of Fig. 22 matches the theory.

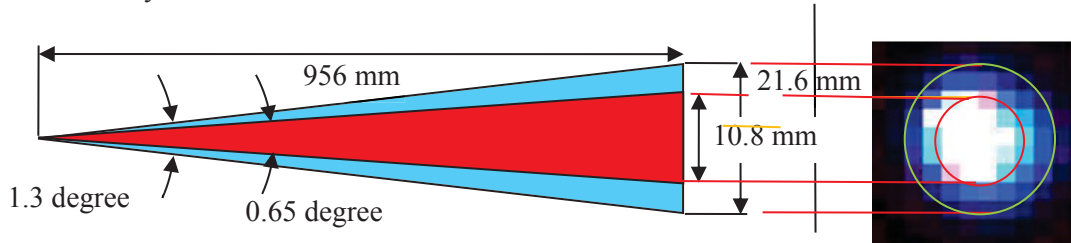


Figure 21: Geometry of the measurement setup for the 1 deg. lens (with $df = 12.7$ mm). While the three bands are equally present in the middle of the FOV, the outer ring is dominated by short wavelength.

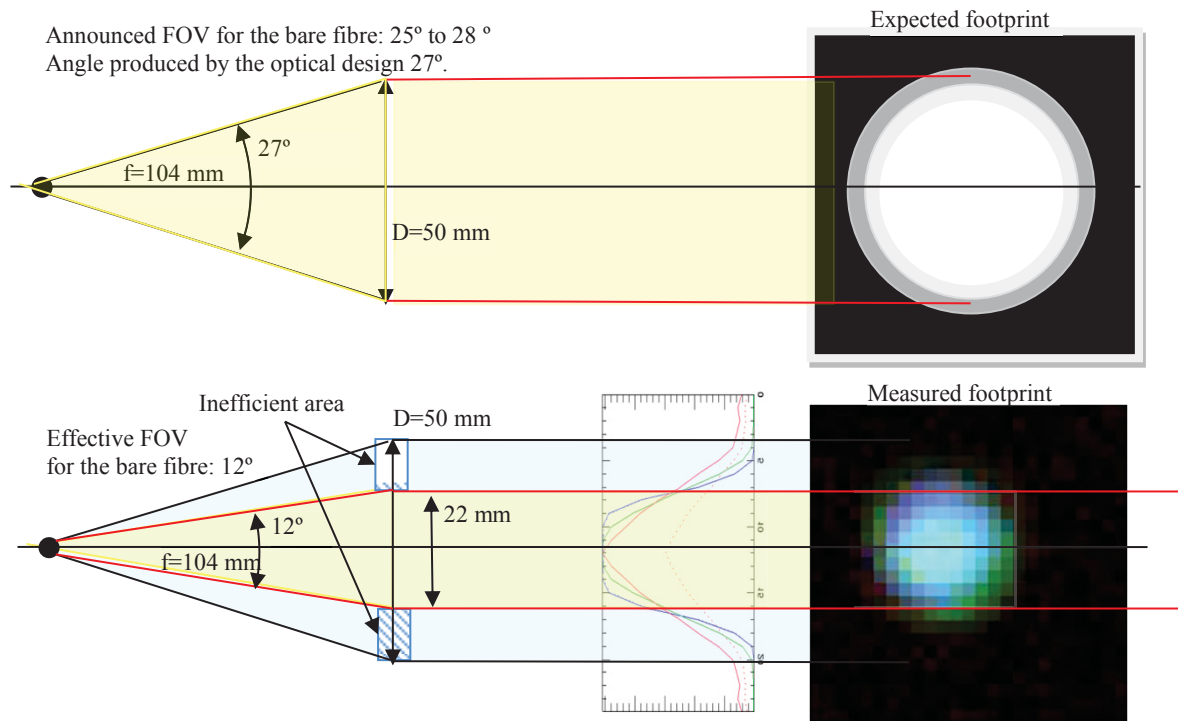


Figure 22: Effect of the FOV of the bare fibre located at the focal point of the entrance optics on the resulting footprint.

8 Measurement of the 1 deg. FOV telescope of the ASD-6175 spectrometer

The 1 deg. telescope was also tested. We had great expectations for this optic because of the achromatic properties of the mirror. Focused and out of focus images are presented in Fig. 23. Other measurements are presented in Annex D.

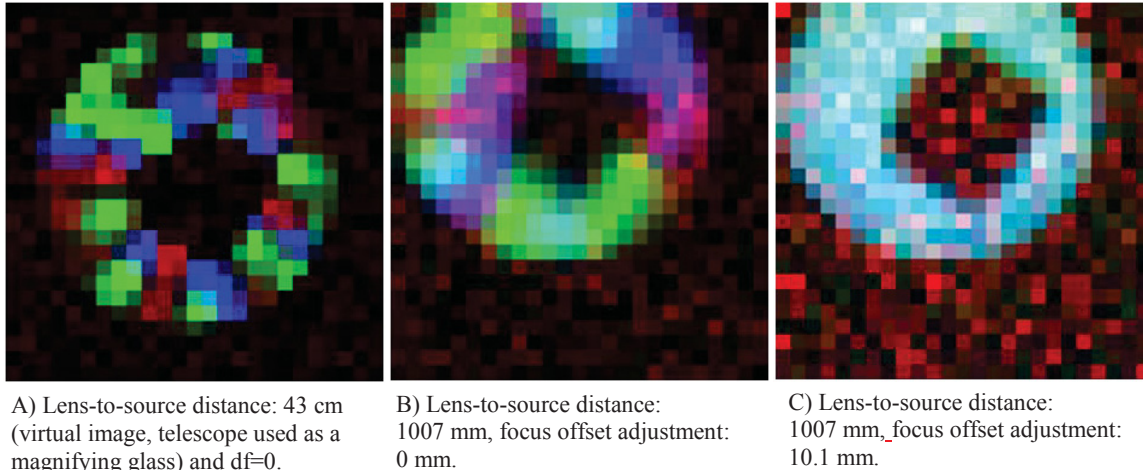


Figure 23: focused and out of focused images produced with the 1 deg. FOV telescope.

When the image is well focused (Fig. 23B), each optical fibre sees a different element of the scene. Otherwise, when the telescope is appropriately defocused (Fig. 23C), the spectral response of the FOV becomes very uniform. A mirror does not have spectral dispersion like a lens.

Fig. 23 also indicates that the real mirror focal length is shorter than expected and is inaccessible, inside the lens tube. Thus, the default optical fiber position at $df=0$ already probes an out of focus image. We had to bring the source at a distance of 43cm to find the image plane.

We however note that the secondary mirror always creates an obscuration in the FOV. Considering Fig. 24, this blind spot is something normal at close range. Such telescope design is not intended for measurement at close range. However, the size of the observed blind spot, with an object distance of approximately 1m, remains bigger than calculated in Table 4. The pupil effect of the optical fibre (Fig. 25) is also responsible for this obscuration which is larger than the simple geometric estimation of Fig. 24 and Table 4.

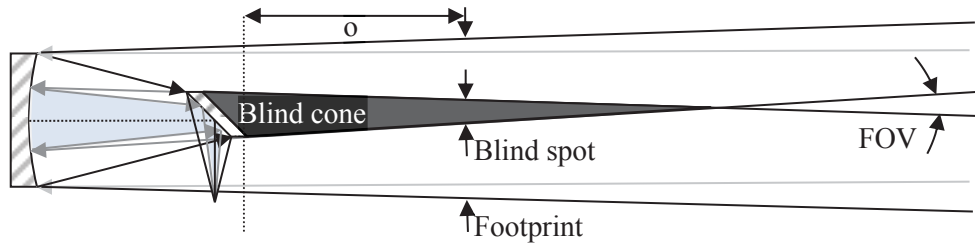


Figure 24: Blind spot produced by the obscuration caused by the secondary mirror.

Figure 25 shows the telescope design with approximately the real dimension of the optical elements and focal length. For this Newtonian telescope, the internal conical FOV sustained by an ideal detector is approximately 28 degrees (between the detector and the primary mirror). This is a good match for the supposed 25 degrees of the bare fibre. Therefore, the optical fibre should be able to see the primary mirror entirely. However, Fig. 12 indicates that the real effective FOV is only 12 degrees. By drawing this 12-degree cone in the optical design, Fig. 25 shows us that the effective section of the primary disk that is seen by the fibres is (almost only) the section that is obscured by the secondary mirror. This optical design produces a reading because the optical fibre has still 15% of sensitivity in the halo between 12 and 25 degrees (see profiles of Fig. 11).

Table 4: Calculated foot print and blind spot dimensions in relation with the object distance.

P=Primary mirror : 50 mm S=Secondary mirror : 16 mm f: 100 mm detector size (at focal plane) : 1.7 mm FOV: 0.9 deg.		
O: Object distance (mm)	Blind spot diameter (mm) = $S - 2 O \tan (FOV/2)$	Foot print diameter (mm) = $P + 2 O \tan (FOV/2)$
1000 mm	0	66.4 mm
750 mm	3.7 mm	62.3 mm
430 mm	7.8 mm	58.2 mm

In conclusion, this design is not very efficient. The secondary mirror obscures the image area where the detector is the most sensitive (central FOV corresponding to the 12 bare fibre FOV) and the blind spot cannot be removed at close range. Only an off-axis telescope could solve this problem.

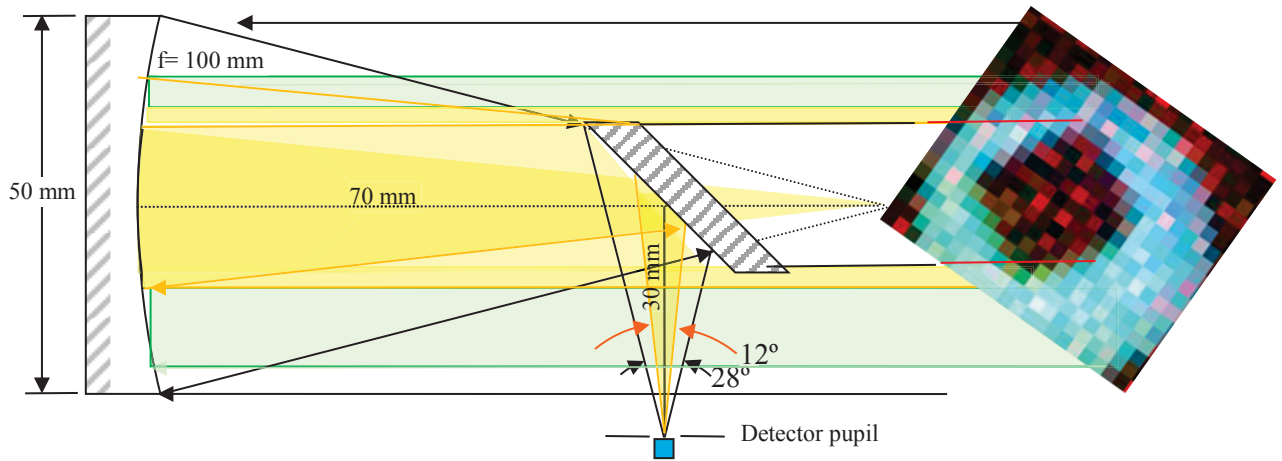


Figure 25: Effect of the limited FOV of the optical fibre placed in the detector pupil.
 Green: output beam for a 28° FOV optical fiber,
 Yellow: output beam for a 12° FOV optical fiber

9 Measurement of the FOV of an off-axis mirror

We believe that a reflective optic is the best solution for getting a uniform spectral response for the goniometer optic. But, the Newtonian design is not adequate. If the uniform FOV of the right image of Fig. 23 could be obtained without the blind spot, this would be the ideal optic for the goniometer. An off-axis (primary) mirror could do that. With an off-axis mirror, the secondary mirror (if it is required) is not in the path of the entering light beam. It does not create an obscuration effect.

To test this, an off-axis mirror, that was available in the laboratory, was used. However, it did not have the desired proprieties (off-axis values too great) but it was possible to acquire images without blind spot. But the very short focal length ($f/\text{number}=1$) and off-axis exaggeration (70 degrees) made a very deformed PSF (point spread function) and the illumination of the head of the optical fibre bundle was not uniform. Figure 26 illustrates the use of this off-axis mirror.

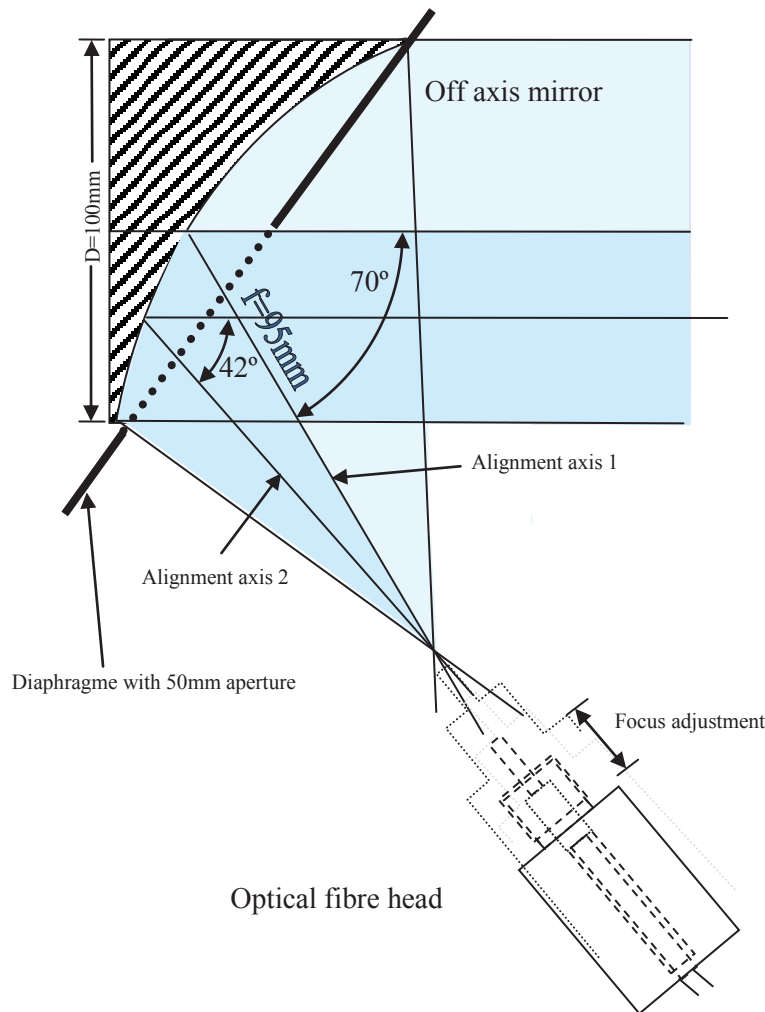


Figure 26: Measurement of the FOV of an off-axis mirror restricted to the 42 deg. off-axis zone.

This mirror was use at full aperture and with an iris which has half the mirror size. This is equivalent to comparing two different mirrors. With the iris, the f/number is 2 (rather than 1) and the off-axis angle is reduced from 70 degrees to 42 degrees. This is a 50 mm f/2 telescope like the one of the previous Chapter, but without secondary mirror and there is no more central dark spot in the scanned FOV.

When the image of the light source is perfectly focused, both scans (with and without iris) are similar and present spectral irregularities. When the image is defocused, the smaller mirror (i.e., with the iris) has better performance. It is less affected by coma aberrations. But Figure 27 shows that the scanned images still suffer from spectral irregularities. This was not expected for a reflective optic. The explanation is presented in Fig. 28.

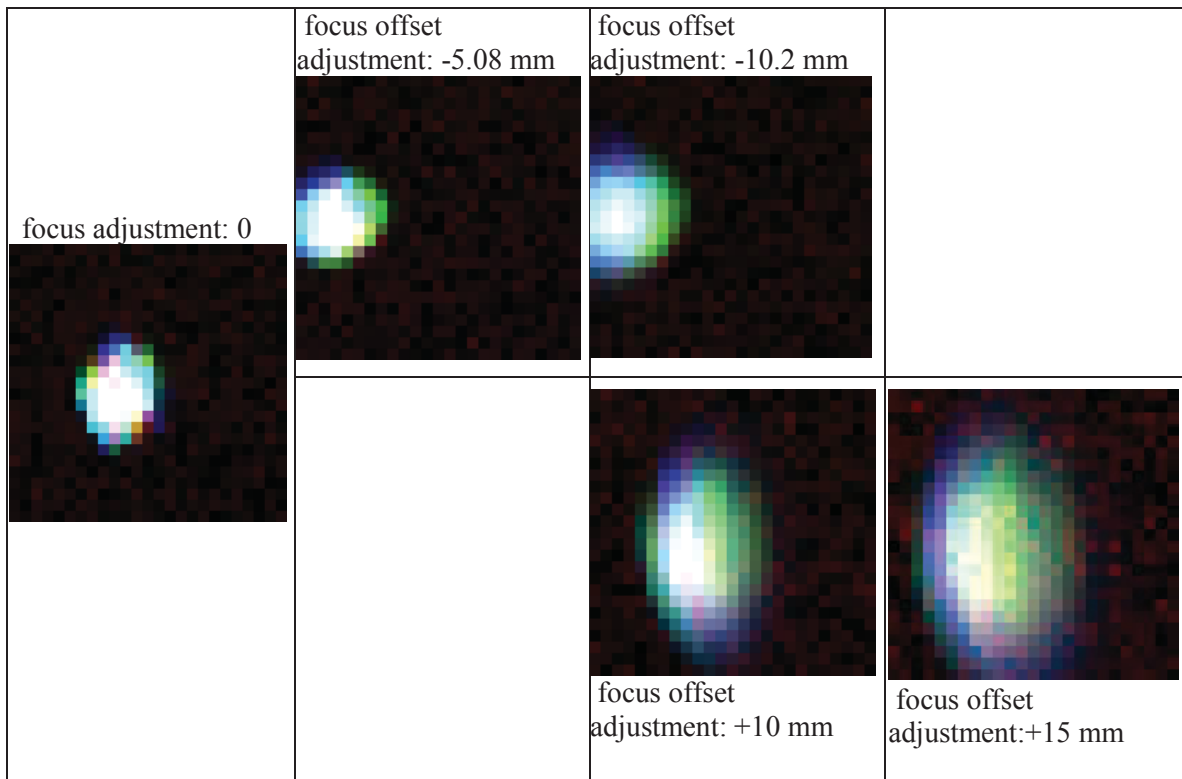


Figure 27: Scans of various defocused images for an object at a distance ($O+f$) of 955 mm from the off-axis mirror.

The drawback of this optical system is that, at the focal plane, the energy is not uniformly distributed. Out of focus, the light is spread over a smooth elliptic area with sharp edges. When almost focused, the PSF suffers from strong coma aberration, it is heavily textured and it has spatial spike, like the drawing represented in Fig. 28. The effect of the sharp edge is that only certain fibres are illuminated, causing a band selection. This causes the green and violet dominance effect on the scans of the defocused images. When the focus is well done, the texture PSF illuminates more certain fibres that other and cause a strong color change in the focused image of Fig. 26. To this, the effect of the 12 deg. FOV of the optical fibre also adds strange behaviour to the optic.

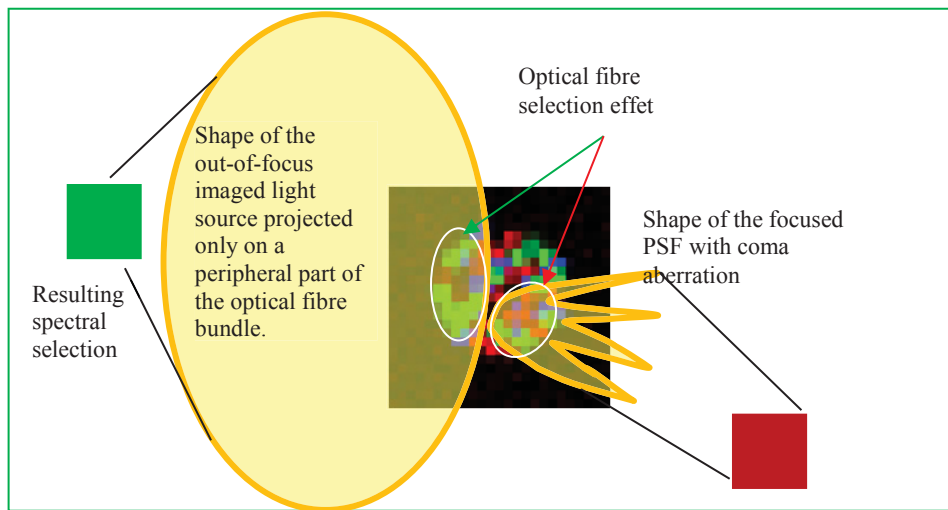


Figure 28: Effect of the partial illumination of the optical-fibre bundle head.

This test is not very conclusive. It suggests that a mirror that produces a smoother PSF must be used. There are several solutions. First, use a higher f/number. Second, use an off-axis closer to the axis (20 to 30 degrees). Maybe a spherical mirror tilted by a few degrees would do the job. This last hypothesis was finally tested and presented in next Chapter.

10 Measurement of the FOV of a tilted 50 mm f/4 spherical mirror

Up to now, the best result (for the FOV uniformity) was obtained with the 1-degree telescope of Chapter 8 (Annex D), except for the central blind spot. Hence, it was decided to try an equivalent off-axis optical design, so the blind spot will not appear.

The telescope of annex D is a f/2 optics. It has an internal conic beam with an angle of convergence of about 25 degrees. In principle, this should be a matched for the 25 degrees bare optical fibre (Fig. 25), such as specified by the company. But, Chapter 5 indicated that the real efficient FOV of the bare fibre is about 12 degrees. Because of this, the fibre sees only the central part of the primary mirror, the area that is also obscured by the secondary mirror (see Fig. 25). Therefore, it is now considered that an f/4 mirror with a convergence angle of 12 degrees (indicated by the red arrows in Fig. 29) is a better match for the FOV of the optical fibre. Also by tilting the primary mirror, the secondary mirror does not obscure the FOV anymore. Because this is not an imaging system, spherical aberrations are not very important, particularly when the optics is used out of focus like in the present case. This is by far less important than the achromatic dispersion cause by a lens, as was shown in Chapter 7. Figure 29 shows the optical design while Fig. 30 shows the Solid Edge design of the component mounted on the scanner mechanism.

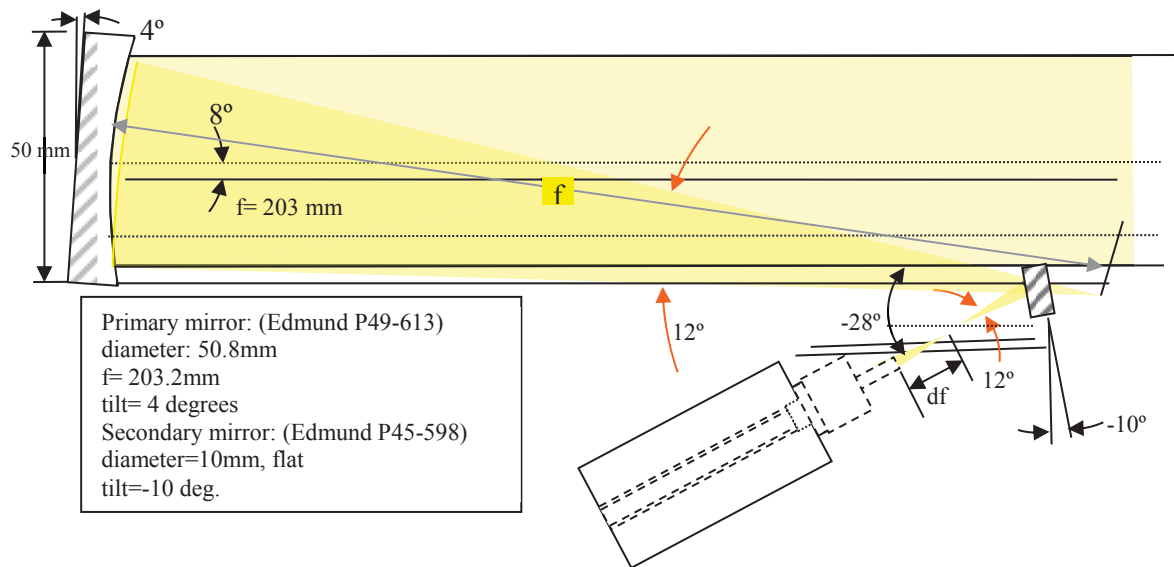


Figure 29: Optical design based on a tilted 50 mm spherical f/4 mirror; the input FOV is 0.5 degree.

With this design, an input parallel beam (for an object at an infinite distance) is focused at $f=203$ mm ($df=0$). For a close object at a distance of 1m, the image plane is $df=40$ mm beyond this point. Considering the size of the optical fibre bundle and the mirror focal length, the calculated FOV divergence is 0.5 degree (see Fig. 5)



Figure 30: Setup with the tilt $f/4$ 50 mm spherical mirror mounted on the scanner.

Figure 31 shows different images obtained by scanning the integrating sphere light source. For the focus adjustment $df=0$, i.e., for an object at the infinite distance, the detector catches only the parallel input beam plus, more or less, the 0.5 degrees of FOV. This scanned area is the most uniform (spectral) input obtained up to date, excepted for the one from Fig. 23c acquired with the 1 degree telescope. But this last one has a major obscuration problem. Other measurement details are given in Annex F.

$df=0$ mm (focused to the infinite, or $df=-40$ mm relatively to the image plane)	$df=20$ (relatively to the focal length)	$df=40$ m (focal length + 40 mm, i.e., focused image plane)	$df=60$ mm

Figure 31: Scans of various defocused images for an object at a distance ($O+f$) of 1.3 m from the tilted spherical mirror 50 mm $f/4$.

11 Tests done with the scrambler device

Analog Spectral Devices, the manufacturer of the ASD spectrometers discussed in this report, offers a device called a “scrambler” that is supposed to make the FOV of the ASD optics more uniform. It is built with a large single optical fibre (1.7 mm of diameter and 76 mm long) that is placed in line with the optical fibre bundle (Fig. 32). When the light propagates inside this fibre, the multiple reflections are supposed to mix the light and destroy the spatial texture of the FOV, making it more uniform. This study would not be complete if such a device were not considered. A few comparative measurements were done to evaluate the scrambler.



Figure 32: Scrambler device place at the entrance of the optical fibre bundle.

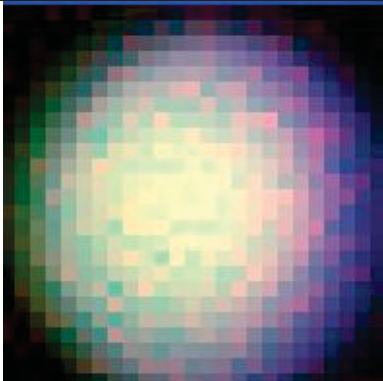
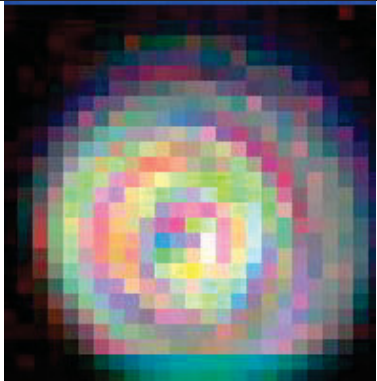
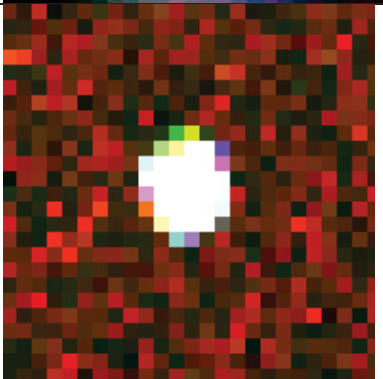
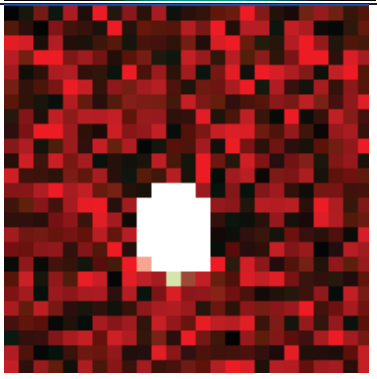
	Without scrambler	With scrambler
df=0, at the mirror focal point.		
df=40 mm, at the focused image plane.		

Figure 33: Evaluation of the scrambler effect with the 50 mm tilted $f/4$ spherical mirror.

The use of this scrambler is not very convincing. In some cases it seems to improve the result, but in other cases it makes thing worst. First of all, it attenuates the signal. But, a defocus also attenuates the signal. When used with the 50 mm tilted mirror (Fig. 33) it produces a better reading for the well-focused image (df=40 mm) where the color effects of the pixels in the

periphery disappear. But this setup will not be used for the goniometer; the footprint is not large enough. For the more uniform and larger footprint, i.e., with the focus adjustment $df=0$; it makes results poorer.

With the standard (COTS) ASD lenses (Fig. 34), the use of the scrambler is not convincing either. With the 1 degree lens, using the default adjustment $df=0$, the FOV is not really improved. For the 8 degrees lens, the FOV texture disappears almost completely, but the signal is highly attenuated. Unfortunately, our current measurements (for the 8 deg. lens with the scrambler) are not very good. It would probably need to be measured again. But, because this 8 degrees lens was not selected for the final goniometer design, based on other consideration, we did not repeat the measurements.

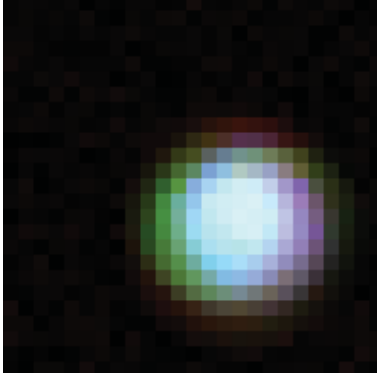
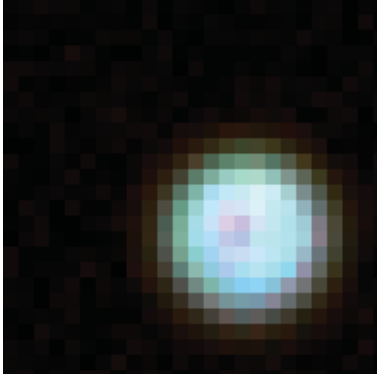
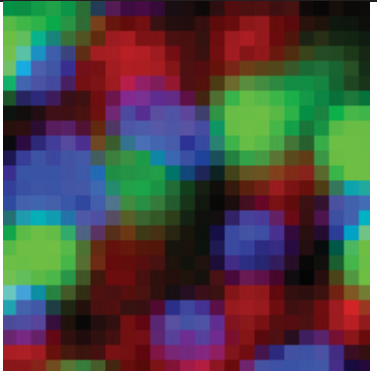
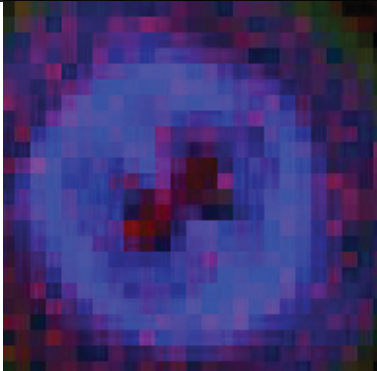
	Without scrambler	With scrambler
1 deg. lens, $df=0$		
8 deg. lens, $df=0$		

Figure 34: Evaluation of the scrambler effect with the ASD 1 and 8 degrees lenses.

In conclusion, the optical scrambler is not a better solution than simply avoiding placing the head of the optical fibre at the well-focused image plane. A defocus is required. By default, for the 1 and 8 degrees lenses, the optical fibre is placed at $df=0$ (at the focal point of the lens), i.e., focused for an object at an infinite distance. For the 8 deg. lens, we recommend introducing a focus offset “ df ” from 7 to 12 mm (Fig. 13). For the 1 deg. lens, the focus offset should be set to $df=12$ mm for the measurement of a far object, or $df=0$ for an object at very close range (avoiding the well-focus image plane at $df=12$ mm for an object at 1 m).

12 Conclusion

This report presents an analysis of the spatial distribution of the field of view of an ASD spectrometer. Several input optics were tested, some COTS and some from an ad-hoc design. These optics were tested with the optical fibre bundle placed at the focal point of the optics, at the image planes and other positions. For a goniometer application, we wish to be able to measure a sample of a reasonable dimension, about 50 mm of diameter, and measure the spectral response with the best spatial uniformity as possible in this area. Here are the conclusions regarding the measurements we performed:

- 1- The total maximum FOV of the bare fibre bundle is around 25 degrees. This is from the leftmost to the rightmost position where a signal can be perceived. However, the real efficient FOV is only 12 degrees. This corresponds to the cone where more than 80% of the signal reading is done. All ASD lens and telescope are conceived with a 25 degrees internal conic angle for the focus beam, concentrating the light on the optical fibre. Because of this, the ASD lens and telescope are $f/2$ optical elements. Taking into account the effective 12-degrees FOV, $f/4$ optical systems are more appropriate (see Fig. 22, 24 and 25).
- 2- The 8 degrees lens is not suitable for the goniometer. The worst case is when the optical fibre bundle is placed at the image plane (Figs 13 and 14). Then, the FOV is extremely textured; each spectral band sees different scene elements. Even when extremely out of focus, the FOV remains with different spectral dominance in different parts of the FOV.
- 3- The 1 degree lens is not really better. It suffers from severe chromatic aberrations. The FOV is wider in the shorter wavelengths.
- 4- The footprint of the 1 degree lens is too small. When this lens is focused to the infinite (for a parallel input beam); the projected beam does not correspond to the geometric projection of the optical input entrance (50 mm). The same explanation about the effective 12 degrees FOV of the bare optical fibre (rather than the 25 degrees) makes the periphery of the 50 mm lens ineffective (Chapter 7). With the ASD design, the FOV of the bare fibre is supposed to be a match with the internal conical (focal) beam of 25 degrees. But, in reality, the real bare fibre FOV limits the lens to $f/4$ (Fig. 22) and the projected footprint to only 22 mm (at 1m) rather than 50 mm.
- 5- The 1 degree Newtonian telescope is less affected by spectral dispersion (chromatic aberration) than a lens. When focused to the infinite (Fig. 23c), the FOV is spectrally uniform. However, such a telescope is not suitable for the observation of a sample at close range. The sample is inside the blind spot (Fig. 24). This is also an $f/2$ optical system, which makes the thing worst; the effective part of the mirror (sustained by 12-degrees angle, rather than the 25 or 28 degrees angle) is only the central part, i.e., the area that is obscured by the secondary mirror.
- 6- The off-axis parabolic mirror is an interesting alternative to the Newtonian telescope. This allows the displacement of the secondary mirror out of the optical path and prevents the formation of a blind spot. Unfortunately, the tested off-axis mirror was too much

off-axis (70°) and with a too large $f/1$ aperture, producing severe aberrations at the focal plane. Also, when out-of-focus, the illuminated area was highly textured (due to aberrations). This optical design was rejected. But it suggested that the use of a less off-axis mirror or a tilted mirror could be adequate. A 50 mm $f/2$ 30° off-axis parabolic mirror was also tested but rejected for the same reasons. However, a 50 mm $f/4$ tilted spherical mirror achieved good results.

- 7- The results for the 50 mm tilted spherical mirror are presented in Chapter 10. When used out of focus, a spherical mirror is good enough; a parabolic mirror is not required. When the focus is set to the infinite, this optic provided the best footprint (for a close object) we measured with all tested optics. It demonstrated that an $f/4$ optic is a better match for the optical fibre placed at the focal point than larger $f/2$ optics. We also believe that an $f/8$ optic could produce an even more uniform FOV, but the total size (longer focal length) of the component could also become an inconvenience. This optical design is the one we selected for the future goniometer.
- 8- Figure 16 indicates that the rotation of a textured sample can simulate a spatial averaging and enhance the goniometer measurements. The use of an optical rotator is not recommended for two reasons; 1) this is a cumbersome piece of equipment which would make the goniometer harder to manipulate and 2) it cannot be used with polarimetric measurement (because of the several internal reflections which alter the light). On the other hand, a sample of small dimension can be rotated in its holder. If required, this approach will be included in the goniometer design.
- 9- The scrambler device was tested. Its performances are not better than simply defocusing the optic.

Based on these measurements, here are some general conclusions. Regarding the question whether it is better to place the optical fibre head at the primary focal of the optical system or at the well-focused image plane, it depends on what is measured. For the first case, i.e., for the measurement of a very small uniform sample, it is tempting to place the fibre head in the image plane; this will produce the maximum sensitivity for a very small footprint, avoiding measuring the surrounding background. But, in this case, there is a high risk that the sharp focused spot does not illuminate uniformly all the optical fibres and involuntary forms an unbalanced spectrum. This effect is illustrated in Fig. 28. This effect of unbalanced bands (color effect) is visible in the periphery of all well-focused images presented in this report. Hence, it is always a good idea to introduce a defocus to attenuate this effect. For the other case, i.e., for the measurement of larger and possibly textured samples at close range, large enough to overlap the footprint, it is better to place the fibre head at the optic focal point; this will 1) sense only the input parallel beam (plus the optic divergence, i.e., the lens FOV), 2) provide the best angular resolution for the BRDF measurements, produce a constant footprint and 3) provide the most uniform spectral reading of the sample.

In summary, for the goniometer application, these experiments show that the best optical system should be based on a mirror (i.e., with no chromatic aberration where the width of the FOV does not change with the wavelength), used in an off-axis configuration (no blind spot) and with a focus set to the infinite for the reading of a sample at close range. This provides the required defocus to obtain a spectrally uniform FOV.

References

- [1] Shell J. R., “Bidirectional Reflectance: An Overview with Remote Sensing Applications & Measurement Recommendations”, Center for Imaging Science (CIS); Rochester Institute of Technology; Rochester, New York, May 2004.
- [2] Biliouris D., Verstraeten W. V., Dutré P., Van Aardt J.A.N., Muys B., Coppin P., “A Compact Laboratory Spectro-Goniometer (CLabSpeG) to Assess the BRDF of Materials. Presentation, Calibration and Implementation on *Fagus sylvatica* L. Leaves”, *Sensors* 2007, 7, pp. 1846-1870.
- [3] Milton, E. J. et al., *Progress in field spectroscopy, Remote Sensing of Environment* (2007), doi:10.1016/j.rse.2007.08.001, <http://linkinghub.elsevier.com/retrieve/pii/S003442570700363X> (last accessed June 2011).
- [4] Mac Arthur A., MacLellan C., Malthus T. J., “Determining the FOV and directional response field spectroradiometers”, *Proceedings 5th EARSeL Workshop on Imaging Spectroscopy*. Bruges, Belgium, April 23-25 2007.
- [5] MacArthur, A., MacLellan, C., & Malthus, T. J. (2006). What does a spectroradiometer see? *Proceedings of the Annual Conference of the Remote Sensing and Photogrammetry Society*. Cambridge, UK Remote Sensing and Photogrammetry Society.
- [6] ASD field portable spectroradiometer; <http://www.asdi.com/products/instrumentation>.
- [7] SVC field portable spectroradiometer, GER series; <http://www.spectravista.com/>.
- [8] Lévesque M. P., Maj. Bedard D., Giroux S., Wallace B., “Measurement of the photometric and spectral BRDF of the CanX-1 satellite engineering prototype: Experimental setup and measurement procedures”, TR-2013-441.
- [9] Dangel S., Verstraete M.M., Schopfer J., Kneubühler M., Schaepman M, Itten K.I., “Toward a Direct Comparison of Field and Laboratory Goniometer Measurements”, *IEEE Trans. on Geoscience and Remote Sensing*, Vol. 43, No. 11, Nov. 2005, pp. 2666-2675.
- [10] Baribeau R., H, “Reflecting on colour”; <http://www.nrc-cnrc.gc.ca/eng/news/nrc/2009/04/06/gonioreflectometer.html> (last accessed: 01 Feb 2011).

Annex A Band selection

The ASD spectrometer produces output spectra with 2151 spectral wavelengths (1 nm sampling), separated into three wavebands read by three different detectors or spectrometers (Fig. 3). Their band distributions are listed in Table A1. The wavelength separation between two consecutive channels is 1 nm. However, the bandwidth of these channels is larger and they overlap each other (bandwidth: 4 to 12 nm, depending of the wavelength).

Table A1: Spectral band associated with each detector

	First band number (wavelength in nm)	Last band number (wavelength in nm)
VNIR Detector	1 (350)	621 (970)
SWIR 1 Detector	622 (971)	1411 (1760)
SWIR 2 Detector	1412 (1761)	2151 (2500)

All these wavelengths are not equally sensitive. The first wavelengths (350 nm) suffer from a lack of sensitivity, as well as the last wavelengths (2500 nm). Furthermore, the first spectral wavelengths are very sensitive to the light reflected by the optical bench, causing a background gradient in the acquired image. Curiously, this is not visible for longer wavelengths. Maybe the aluminum table is highly reflective at short wavelengths but the most plausible explanation (provide by Chapter 5) is that the fibre bundle has a larger FOV in the short wavelengths and that the reflection by the optical bench is in the FOV for short wavelengths only.

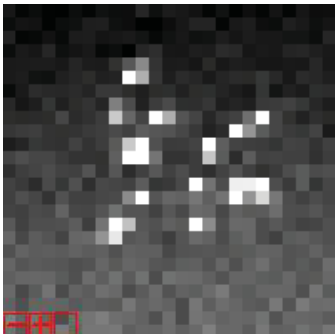
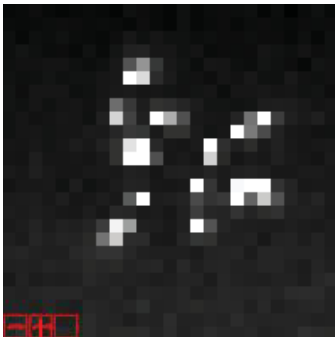
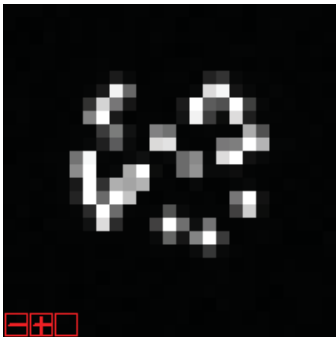
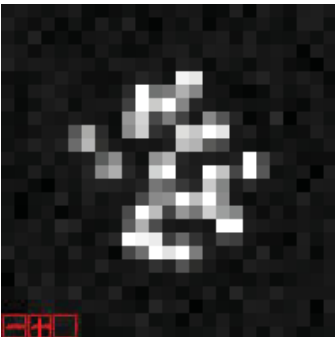
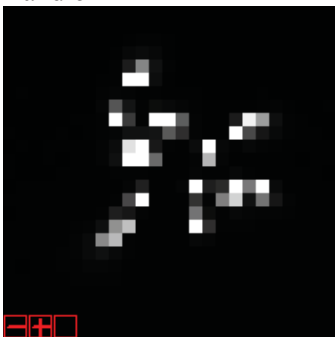
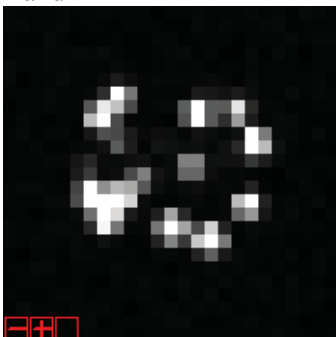
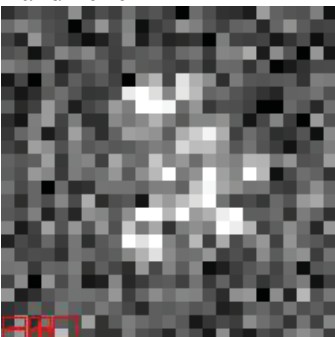
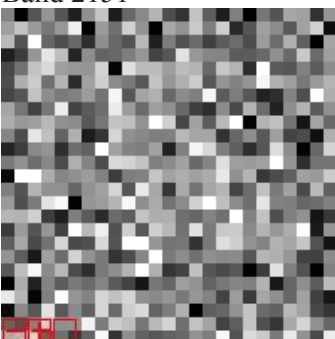
For the analysis of the spectrometer FOV, i.e., the effect of the sampling of the FOV by the three groups of optical fibres, three images with good contrast (from the different detectors) are combined into a single RGB color image (Fig. 9). The selected bands are the ones in the middle of the valid bands. By “valid”, it is understood that the bands with not enough sensitivity are discarded. Table A3 shows some of the acquired image bands. It is clearly visible why some bands are ignored. The selected bands (presented in Fig. 9, in Chapter 4), used to produce the composite RGB image, are listed in Table A2.

Table A2: Selected bands

RBG component	Band number	Wavelength (nm)
Red	1720	2069
Green	1015	1363
Blue	325	674

All the subsequent analyses are done using always these bands.

Table A3: Scanned images for some specific bands

	Spectral band 1	Spectral band 2	Spectral band 3
Low sensitivity and severe environment reflections	Band 1 		
Good sensitivity, efficient band	Band 30 	Band 622 	Band 1412 
	Selected at mid-range : band 325	Selected at mid-range : band 1015	Selected at mid-range : band 1720
	Band 621 	Band 1411 	Band 2020 
Low sensitivity			Band 2151 

Annex B Measurement of the ASD-6175 8 degrees FOV lens used with the ASD-6175 spectrometer

The 8 degrees FOV lens was measured with several focus offset adjustments (Table B1 to B7). For the object distance $D=O+f=f$ 298 mm, the image is well focused when the optical fibre head is mounted 1.27 mm behind the normal mounting position (Table B2).

Table B1: Measurement of the FOV of the 8 deg. lens, lens-to-source distance: $O+f=298$ mm, focus offset adjustment: $df=0$ mm (supposedly focus to the infinite).

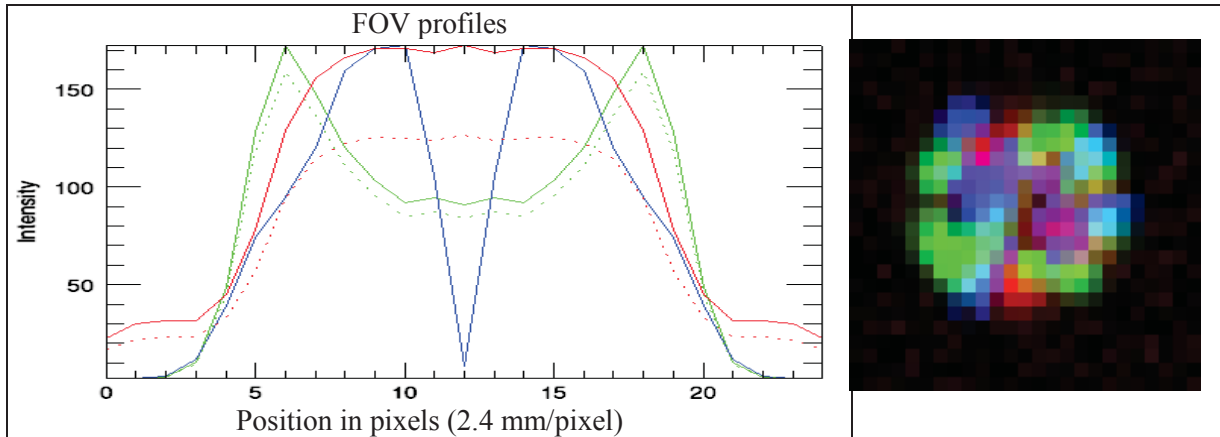
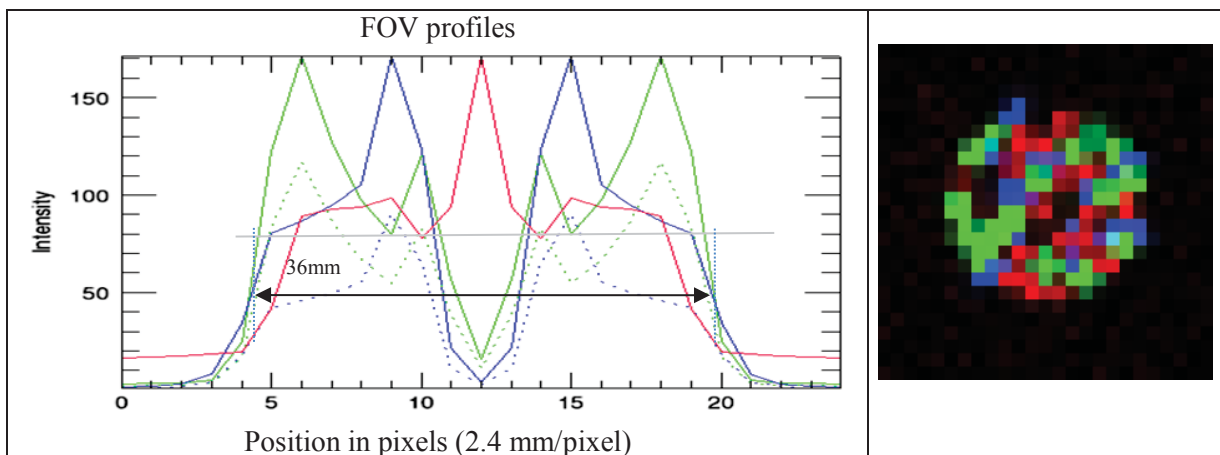


Table B2: Measurement of the FOV of the 8 deg. lens, lens-to-source distance: $O+f=298$ mm. The focus offset adjustment: $df=1.27$ mm (0.05 inch) produced the sharpest image. With the image plane is 0.45 mm behind the focal point, the real calculated focal length is 11.41 mm.



The initial intention, with this optical design, is placing the optical fibre at the focal point ($df=0$) of the lens for an observed object which is at an infinite distance ($O=\infty$). Also, from the

mechanical measurement of the lens mounting, the first estimation of the focal length is $f_0=10.6$ mm (Table 1).

Now, considering a $df=1.27$ mm ($A=df+f_0=11.87$ mm) for an object distance ($D=f+O$) of 298 mm, the relation $f=AD/(A+D)$ of Fig. 4 provides us with a better estimate of the focal length of 11.41 mm. With these new values, we get:

$$A=i+f=0.45 \text{ mm} + 11.41 \text{ mm}=11.86,$$

rather than the first estimation

$$A=df + f_0=1.27 \text{ mm} + 10.6 \text{ mm}=11.87 \text{ mm}.$$

Therefore, when the optical fiber is normally mounted in the mechanical support at a distance of 10.6 mm behind the lens, and that a very far object produces a focused image at 11.41 mm behind the lens, by default this system is defocused by $df=-0.8$ mm. This is not the intention of the original design, but this is not a bad thing because this produces a desired defocus (but not intentional).

Table B3: Measurement of the FOV of the 8 deg. lens, lens-to-source distance: $O+f=298$ mm, focus offset adjustment: $df=2.54$ mm (0.1 inch).

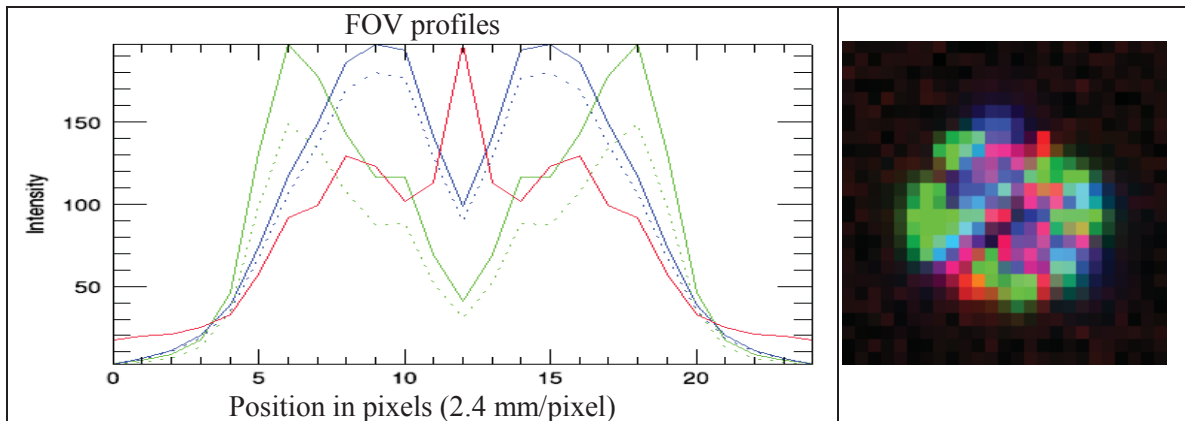


Table B4: Measurement of the FOV of the 8 deg. lens, lens-to-source distance: $O+f=298$ mm, focus offset adjustment: $df=3.81$ mm (0.15 inch).

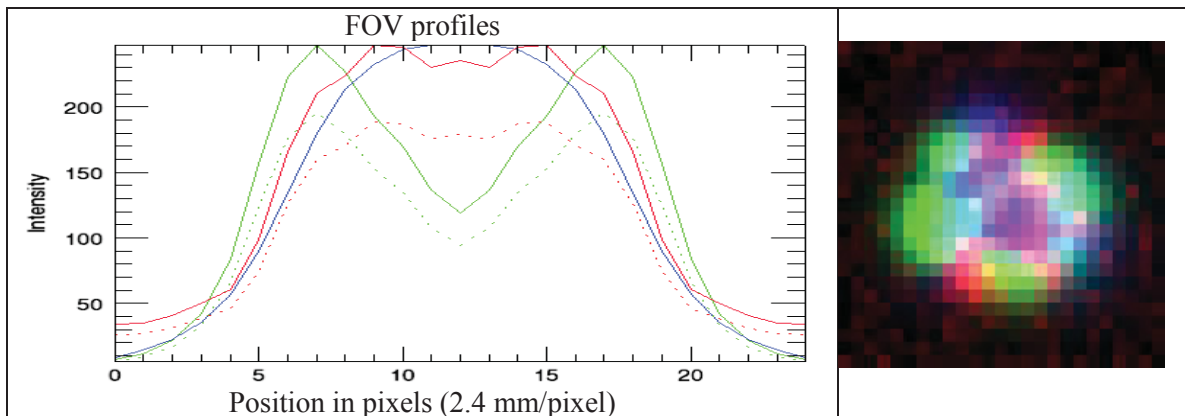


Table B5: Measurement of the FOV of the 8 deg. lens, lens-to-source distance: $O+f=298$ mm, focus offset adjustment: $df=5.08$ mm (0.2 inch).

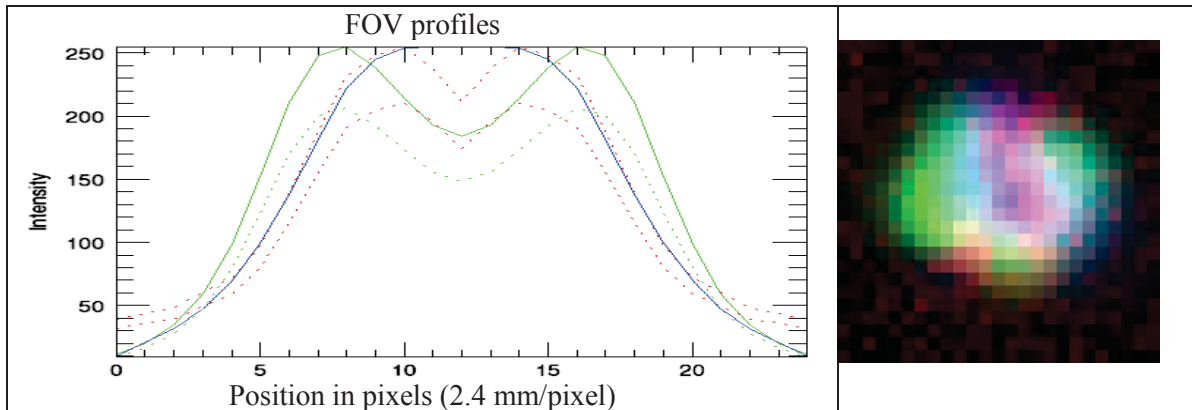


Table B6: Measurement of the FOV of the 8 deg. lens, lens-to-source distance: $O+f=298$ mm, focus offset adjustment: $df=6.35$ mm (0.25 inch).

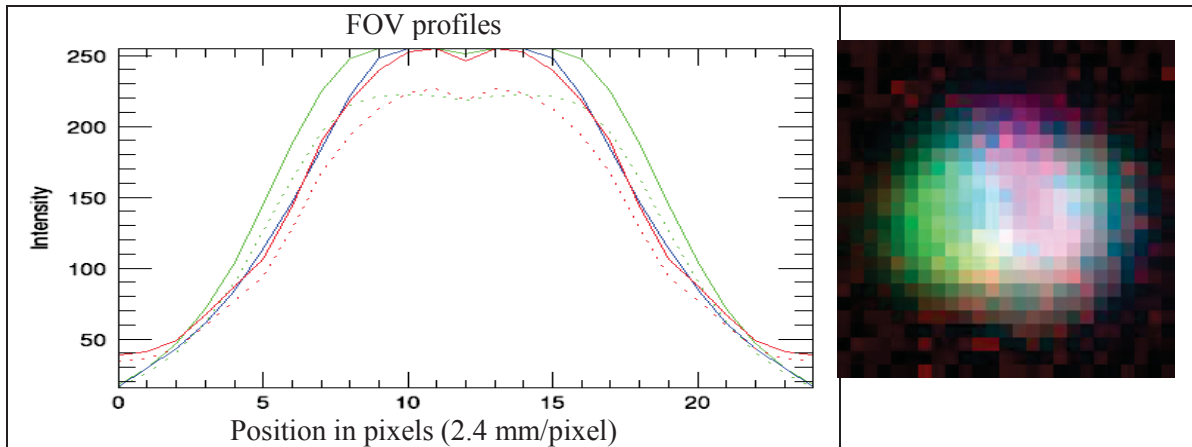
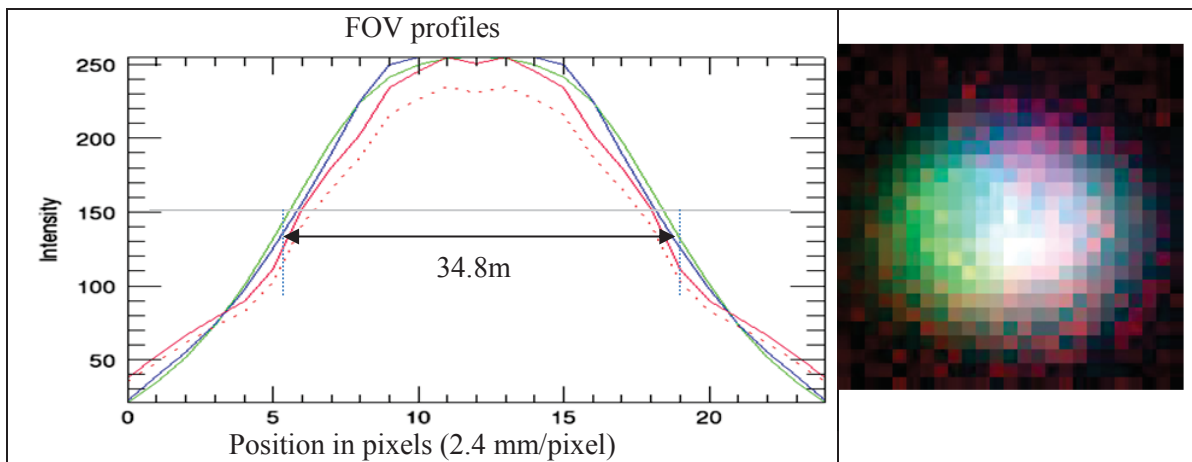


Table B7: Measurement of the FOV of the 8 deg. lens, lens-to-source distance: $O+f=298$ mm, focus offset adjustment: $df=7.52$ mm (0.3 inch).



The FOV was also measured for various object distances (Table B8). The scanned area is constant (6x6 cm, 25x25 pixels). Hence, at a greater distance, a smaller part of the FOV is scanned, causing an apparent zooming effect because the angular pixel FOV is not the same. This is the footprint that is constant.

For an object distance of 1 m, Table B8 shows two images, acquired with and without a diffuser. Even if the diffuser improves the uniformity of the FOV, it does not really solve the homogeneity issue.

Table B8: FOV comparison for two focus offset adjustments and for different object distances. Scanned area: 6x6 cm, pixel footprint=2.4 mm.

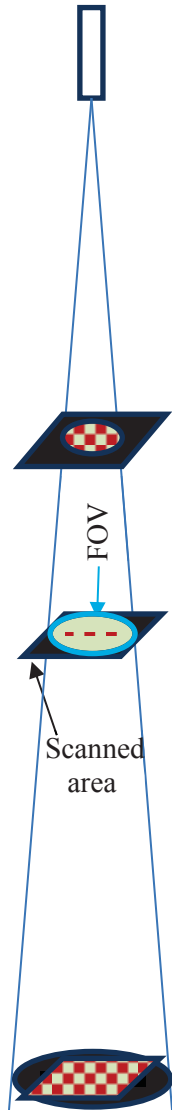
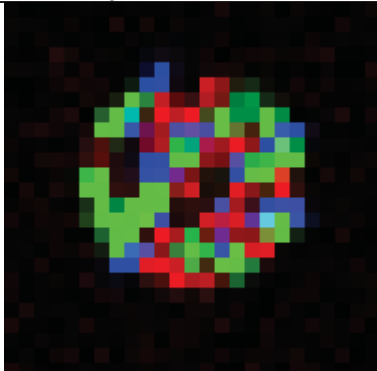
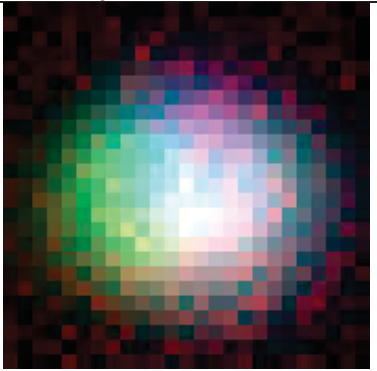
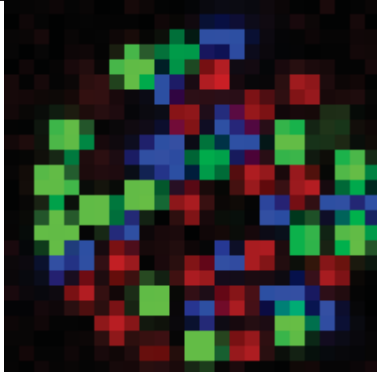
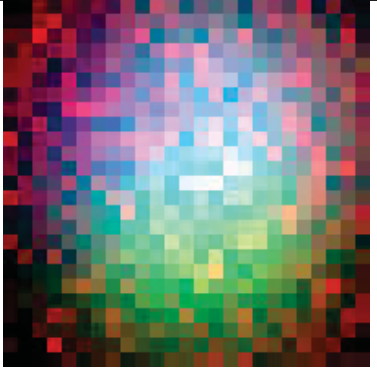
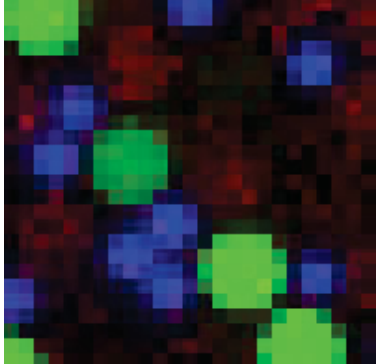

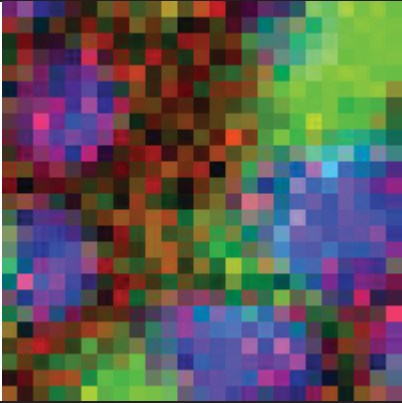
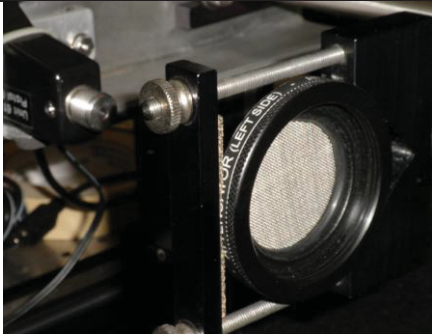
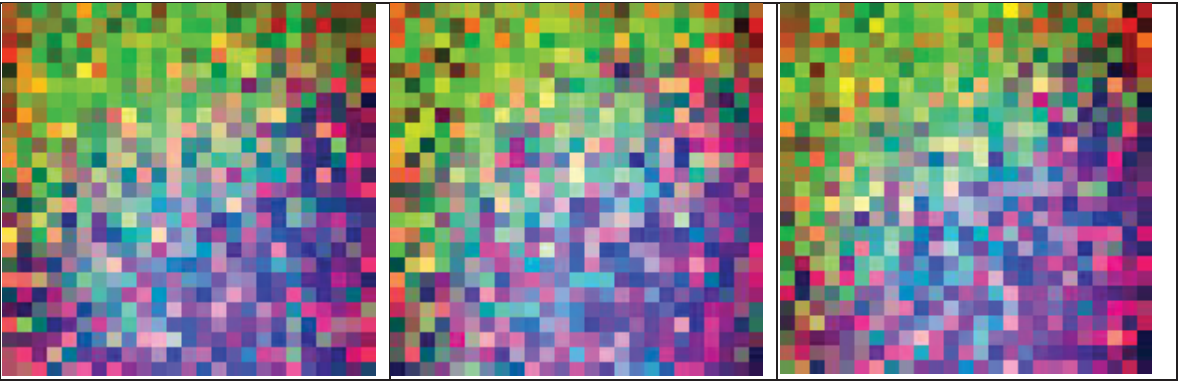
	Focused focus adjustment: $df=1.27$ mm	Out of focus focus adjustment: $df=7.52$ mm	
Lens to object distance: ($O+f$)=298 mm			
Lens to object distance: ($O+f$)=473 mm			
Lens to object distance: ($O+f$)=1 m			

Table B8 (continued)		
Lens to object distance: $(O+f) = 1\text{ m}$, With a diffuser (photo) on the optical fibre head.		 <p>Diffuser in front of the optical-fibre head.</p>

B.1 Sensor scintillation

The defocused image presents exaggerated texture. Several acquisitions were done with the same conditions. The resulting images show texture variations. In conclusion, this is not the optics that is responsible for this texture but the spectrometer sensitivity (sensor noise). In Table B9, the texture pattern is different in all images.

Table B9: Measure of the sensor scintillation (noise). Lens: 8 deg FOV, object distance: $O+f=1\text{m}$, defocus: $df=7.52\text{ mm}$



Annex C Measurement of the 1 degree FOV lens used with the ASD-6175 spectrometer

The following measurements (Tables C1 to C5) are for the lens with the 1 degree of FOV. These measurements show that the lens suffers from a severe chromatic dispersion. Note that the simplest possible lens is desired for a spectrometer. Otherwise, the spectral response would be altered too much. The FOV is approximately that claimed by the company, about 1 degree (Fig. C1). More precisely, it is 1.3 degrees at 325 nm and 0.65 degrees at 1729 nm.

The user of this lens should be aware that, in general, the spectrometer equipped with this lens is more sensitive in the FOV periphery to shorter wavelengths. This could be tricky for the measurement of texture objects.

Table C1: Measurement of the FOV of the 1 deg. lens, lens-to-source distance: $O+f=43$ mm, focus offset adjustment: $df=0$ mm. (supposedly focus to the infinite). This unfocused image is a case of virtual image.

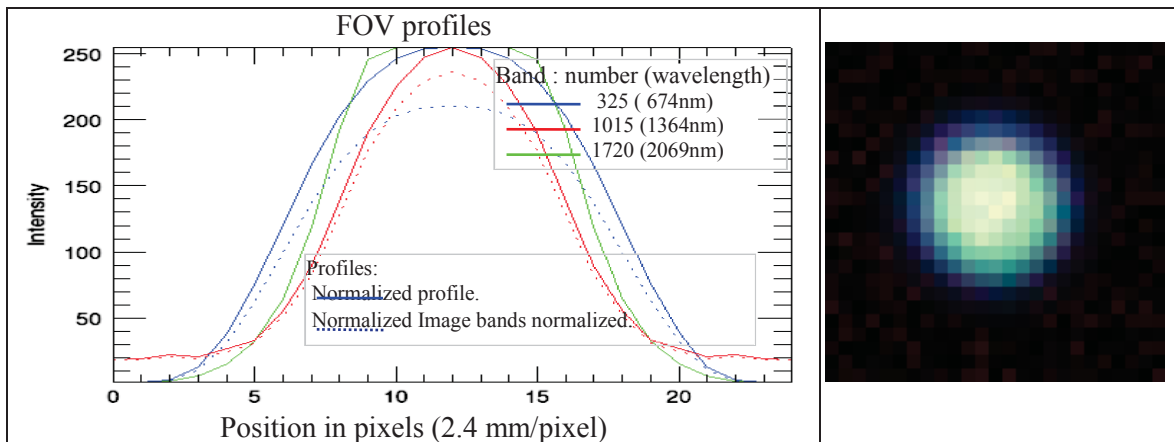


Table C2: Measurement of the FOV of the 1 deg. lens, lens-to-source distance: $O+f=381$ mm, focus offset adjustment: $df=0$ mm (supposedly focus to the infinite).

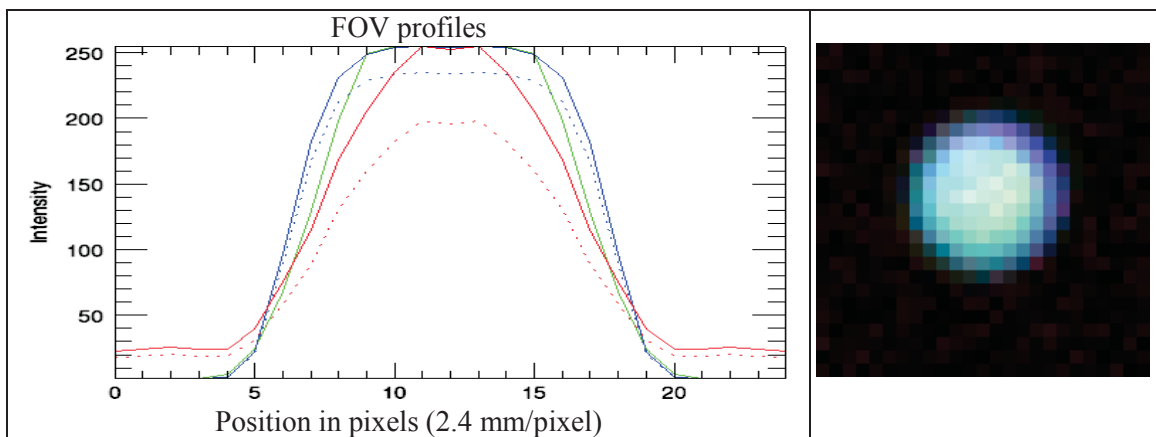


Table C3: Measurement of the FOV of the 1 deg. lens, lens-to-source distance: $O+f=762$ mm, focus offset adjustment: $df=0$ mm. (supposedly focus to the infinite).

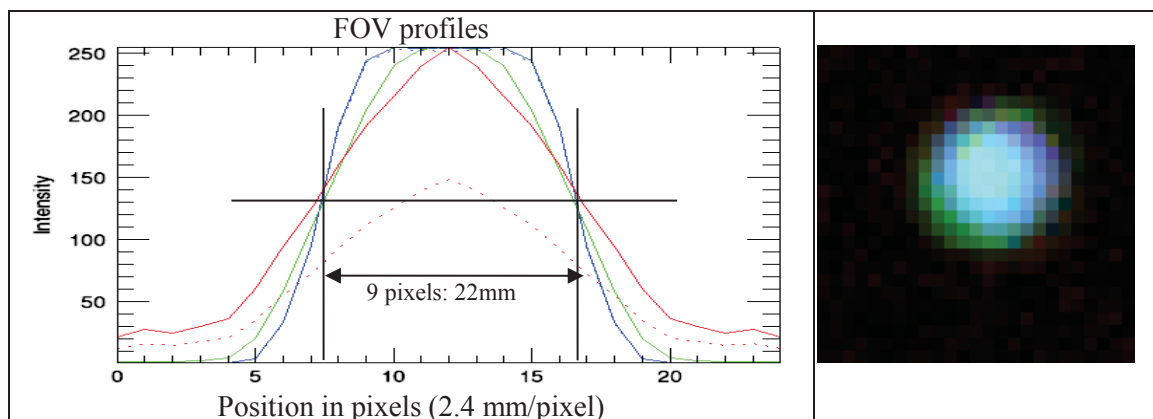


Table C4: Measurement of the FOV of the 1 deg. lens, lens-to-source distance: $O+f=762$ mm, focus offset adjustment: $df=12.7$ mm (0.5 inch). (12.7 mm is the maximum possible refocus; exact focus should be at 16.5 mm).

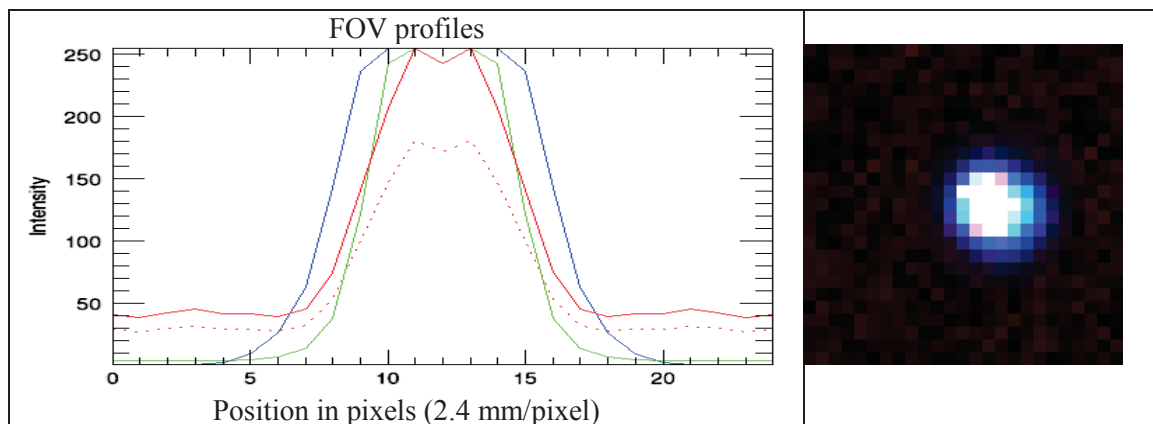
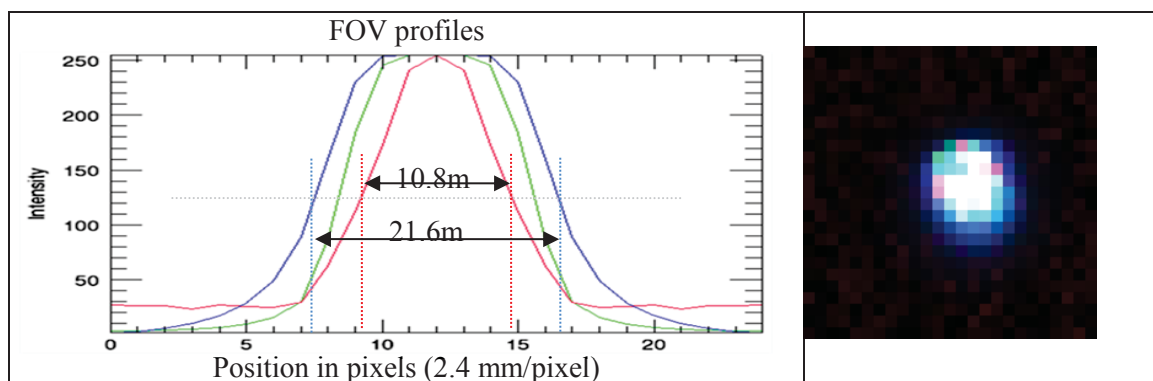


Table C5: Measurement of the FOV of the 1 deg. lens, lens-to-source distance: $O+f=956$ mm, focus offset adjustment: $df=12.7$ mm (0.5 inch).

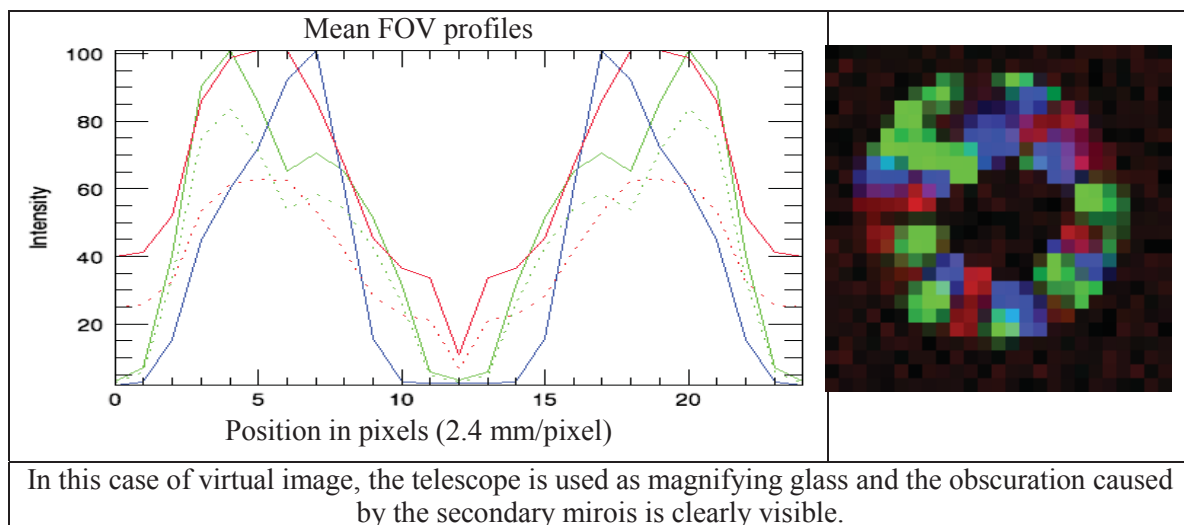


Annex D Measurement of the 1 degree FOV telescope used with the ASD-6175 spectrometer

The following tables contain the measurements for the 1 deg. FOV telescope. By measuring the telescope dimensions, the focal length is estimated to be 107 mm. By placing the light source at 1007 mm, the image plane was expected to be at $df=10.1$ mm behind the focal plane but it was found at $df=0$. This means that the focal length of the primary mirror (Newtonian) is shorter than expected. When observing at great distance, the optical fibre head is normally out of focus.

In every case, the telescope is not adequate for close observation. The secondary mirror produces a blind spot in the middle of the FOV. Normally, for a telescope observing at great distance, the secondary mirror disappears completely in the image, but this is not the case at close range. See Figs. 24 and 25 in Chapter 7.

Table D1: Measurement of the FOV of the 1 deg. telescope, lens-to-source distance: 43 mm, focus offset adjustment: $df=0$ mm (supposedly focus to the infinite).



The exact focal point was searched for (by trying to get a well-defined image) by varying the distance of the source and focus adjustments. It was never found. By moving away the fibre bundle (focus offset adjustment), it was expected to reach the image plane and get a focused image. This was not the case. Then, it was suspected that the optical head was already too far away, i.e., the image plane was inside the telescope tube and inaccessible (for a far object). Then the light source was brought closer (which brings the image plane outside the telescope tube). A better image was obtained for an object distance of 400 mm (Table D2), which, by deduction, means the real focal length is not more than 90 mm (previously estimated at 107 mm). Shorter distances have not been tested. In conclusion, the normal use of this optic, i.e., for object at great distance, makes the optical fibre head already out of focus, which is correct. But the blind spot (cause by the secondary mirror) in the middle of the FOV is always present for close objects and this is a real issue. As explained in Chapter 7, the effective 12 deg. FOV of the bare fibre is responsible for the obscuration zone.

*Table D2: Measurement of the FOV of the 1 deg. telescope:
acquisitions for various distances of the object plane.*

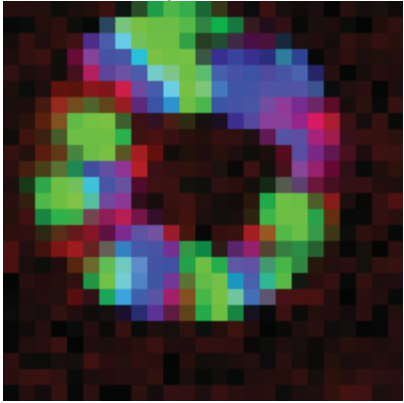
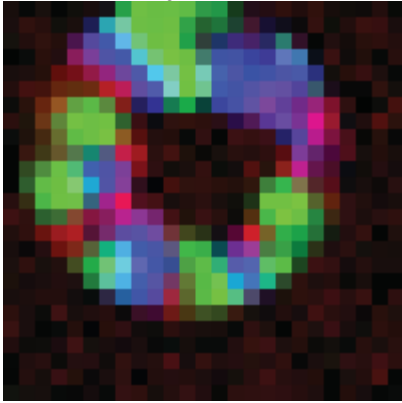
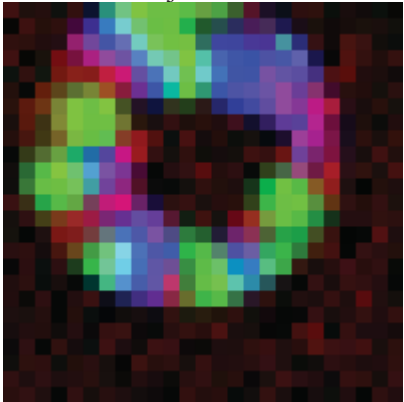
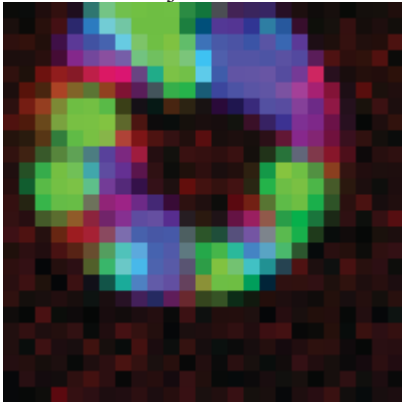
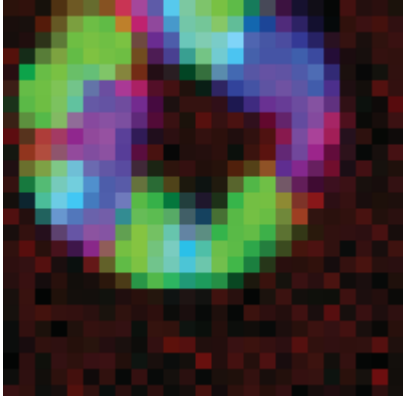
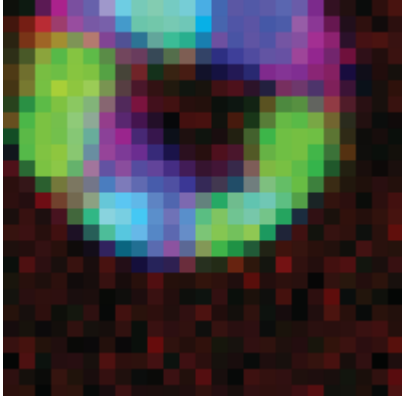
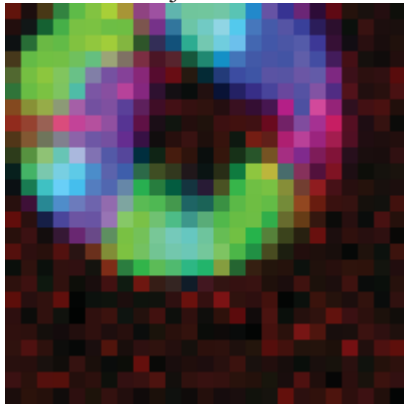
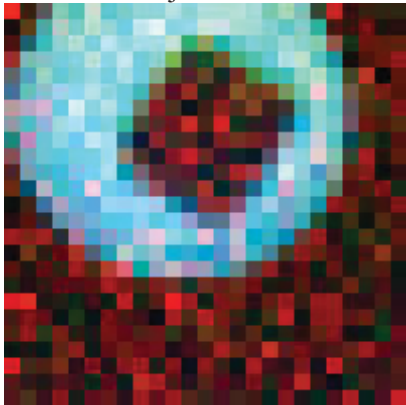
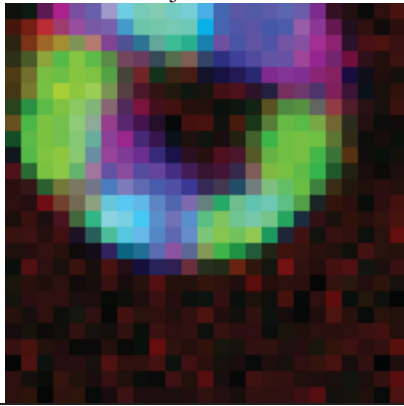
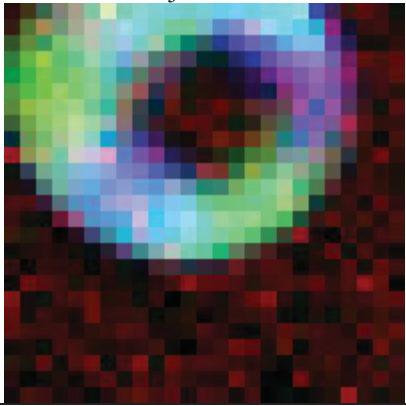
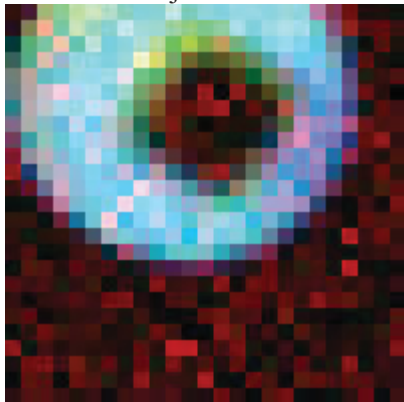
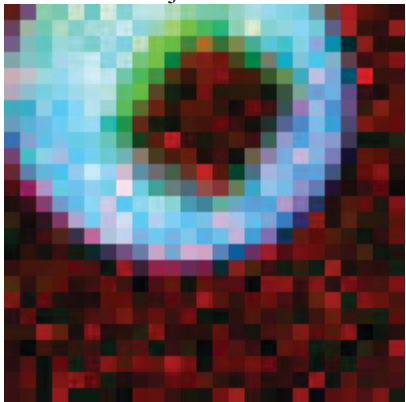
<p>source distance: O=400 mm, focus offset adjustment: df=0 mm.</p> 	<p>source distance: O=500 mm, focus offset adjustment: df=0 mm.</p> 
<p>source distance: O=600 mm, focus offset adjustment: df=0 mm.</p> 	<p>source distance: O=700 mm, focus offset adjustment: df=0 mm.</p> 
<p>source distance: O=871 mm, focus offset adjustment: df=0 mm.</p> 	<p>source distance: O=1250 mm, focus offset adjustment: df=0 mm.</p> 

Table D3: Measurement of the FOV of the 1 deg. telescope: acquisitions for various focus adjustments.

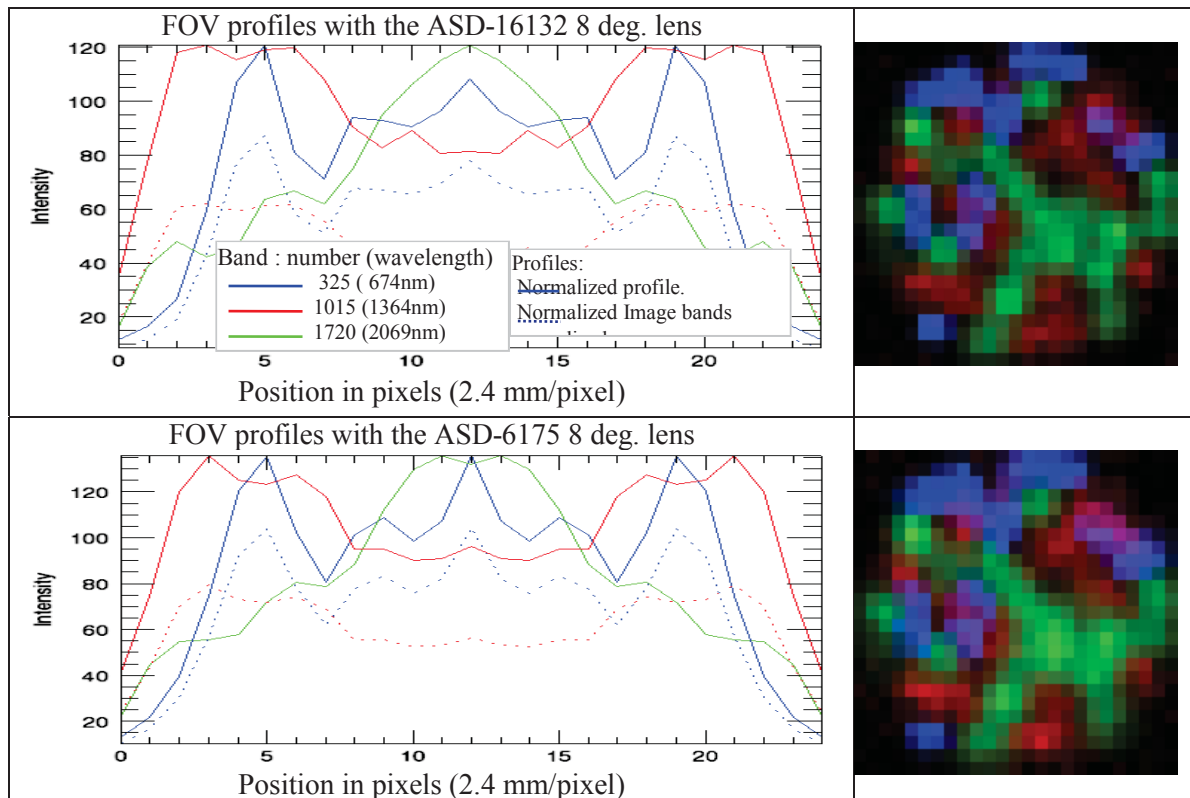
lens –to-source distance: 1007 mm	focus offset adjustment: 0 mm. 	focus offset adjustment: 10.1 mm. 
	focus offset adjustment: 0 mm. 	focus offset adjustment: 1.27 mm. 
lens –to-source distance: 1250 mm	focus offset adjustment: 2.54 mm. 	focus offset adjustment: 5.08 mm. 

Note: The image obtained for O=1007 mm and df=10.1 mm (in Table D3) correspond to the desired FOV. It has a uniform spectral distribution. The only problem is the blind spot. This suggests that by tilting the mirror and use it off-axis an equivalent telescope would fit the requirement.

Annex E Measurement of the two 8 degrees FOV lens (ASD-6175 and ASD-16132 lens) with the ASD-16132 spectrometer

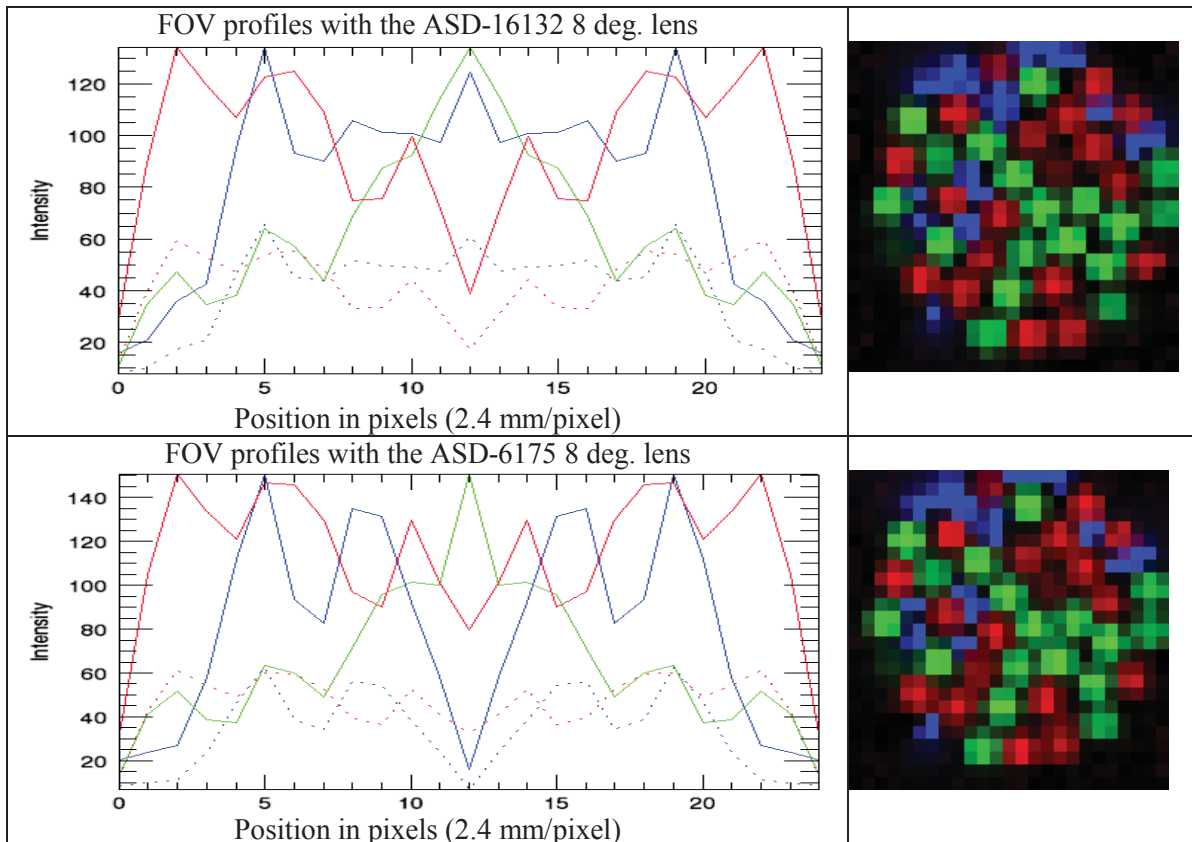
In this series of measurements, the ASD-16132 spectrometer input FOV is measured with the two equivalent 8-degree lenses. The goal is the comparison of the variations due to the optics versus the variations due to the optical fibre bundle differences. Obviously, the optical fibre bundle of the ASD-16132 spectrometer makes a different sampling than the bundle of the ASD-6175. This is shown in Fig. 14 of Chapter 5. Otherwise, this experiment shows that the two lenses are almost identical.

Table E1: Measurement of the FOV of the 8 deg. lens with the field spectrometer ASD s/n 16132. Distance to object plane: $O+f=473$ mm, focus offset adjustment: $df=0$ mm.



In both cases, considering the distance of the light source (473 mm), the focus image should be at 0.2 mm from the focal point. The measurement (Table E2) demonstrated that the real focus is done at 1.27 mm rear of the focal point. This indicates that with the normal utilisation of the ASD, i.e., for measurement of objects at great distance and the optical fibre bundle normally couple with the 8 mm lens, the system is already (slightly) out-of-focus, which is desirable (but a still larger out-of-focus is better).

Table E2: Measurement of the FOV of the 8 deg. lens with the field spectrometer ASD s/n 16132. Distance to object plane: $O+f=473$ mm, focus offset adjustment: $df=1.27$ mm.



Here are other measurements (Table E3 to E5) for the field spectrometer ASD s/n 16132. All the other measurements done in this report are for the field spectrometer ASD s/n: 6175. This illustrates the variation of the spectral distribution in the FOV caused by a different splitting of the fibres in the optical fibre bundle.

Table E3: Measurement of the FOV of the (s/n 16132) 8 deg. lens with the field spectrometer ASD s/n 16132. Distance to object plane: $O+f=473$ mm, focus offset adjustment: $df=5.08$ mm (0.200 inch).

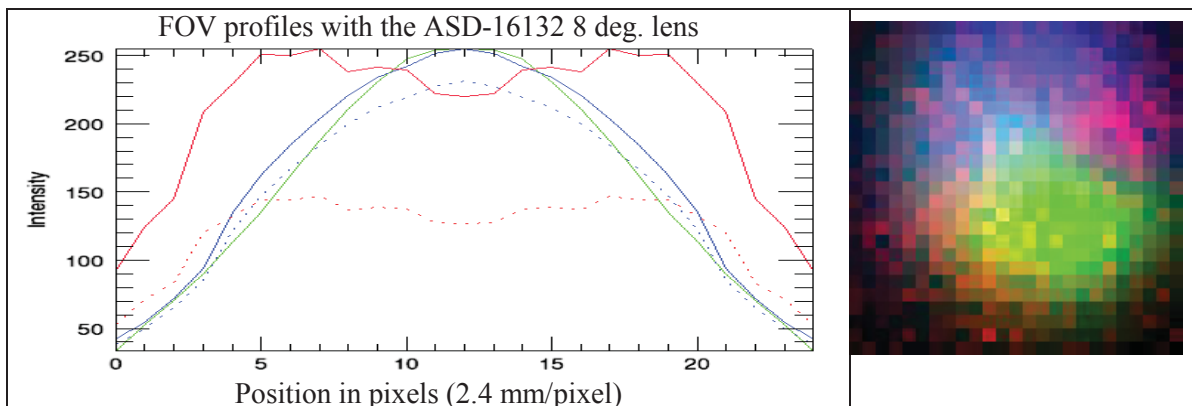


Table E4: Measurement of the FOV of the (s/n 16132) 8 deg. lens with the field spectrometer ASD s/n 16132. Distance to object plane: $O+f=473$ mm, focus offset adjustment: $df=6.35$ mm (0.200 inch).

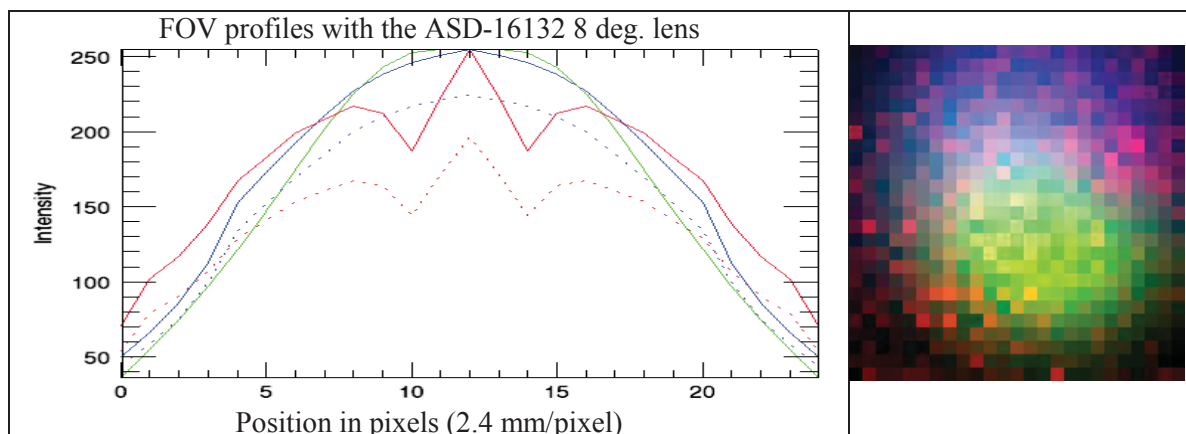
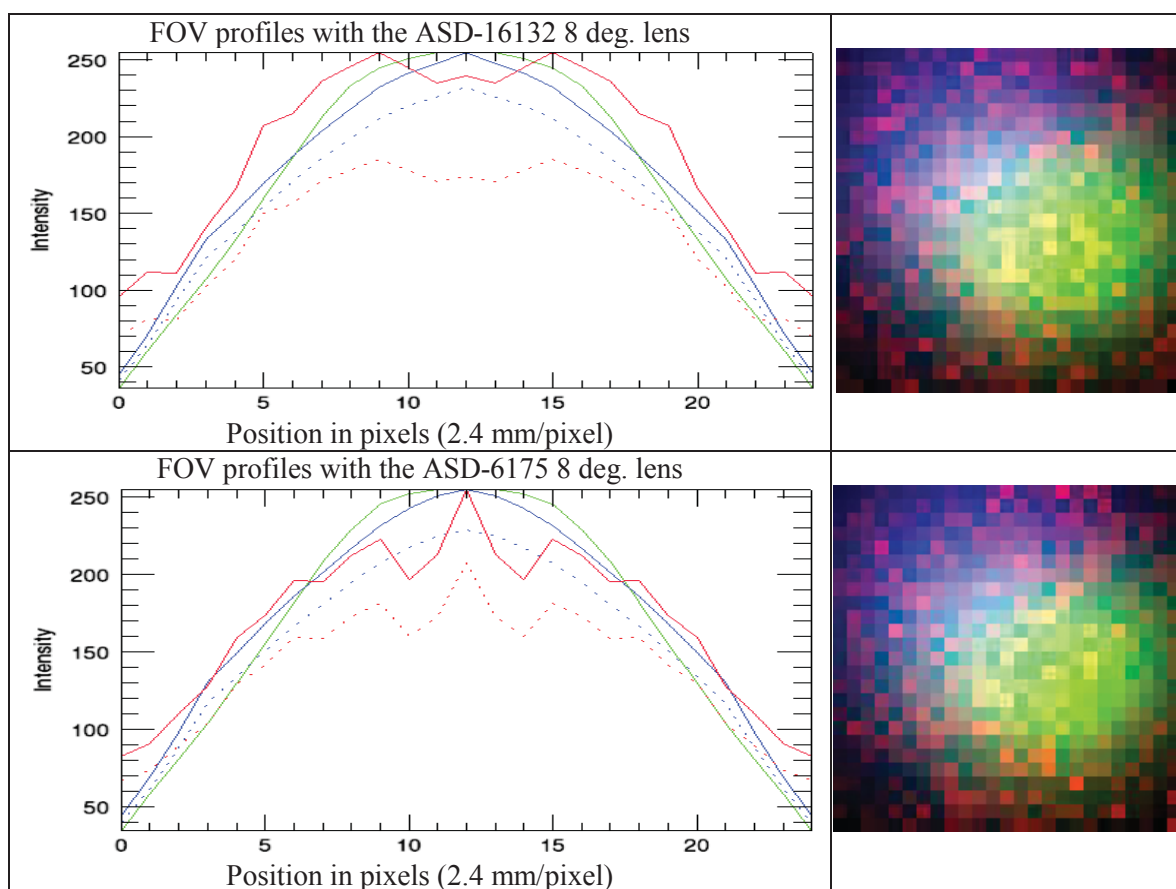


Table E5: Measurement of the FOV of the two 8 deg. lenses with the field spectrometer ASD s/n 16132. Distance to object plane: $O+f=473$ mm, focus offset adjustment: $df=7.62$ mm (0.300 inch).



Annex F Measurement of the FOV of the 50 mm f/4 tilted spherical mirror

Here are all the measurements done with the 50 mm f/4 spherical tilt mirror. By definition, a mirror is achromatic. A spherical mirror suffers from spherical aberrations, but in the case of an out of focus non-imaging system, this is not an issue. The spectral uniformity of the FOV is not perfect, but this is the best we obtained so far.

Table F1: Measurement of the FOV of the tilted 50 mm f/4 spherical mirror. Distance to object plane: $O+f=1500$ mm, focus offset adjustment: $df=0$ mm (focus to the infinite).

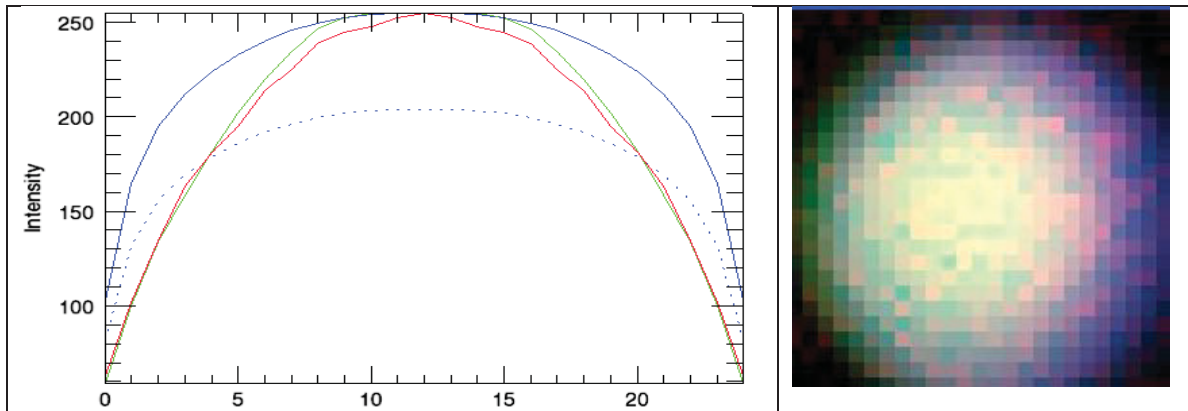


Table F2: Measurement of the FOV of the tilted 50 mm f/4 spherical mirror. Distance to object plane: $O+f=1500$ mm, focus offset adjustment: $df=10$ mm.

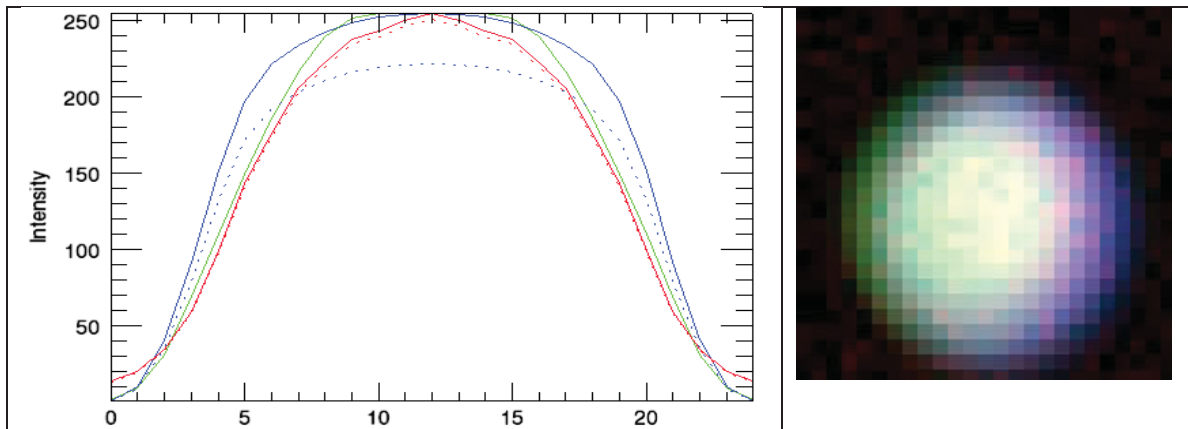


Table F3: Measurement of the FOV of the tilted 50 mm f/4 spherical mirror. Distance to object plane: $O+f=1500$ mm, focus offset adjustment: $df=20$ mm.

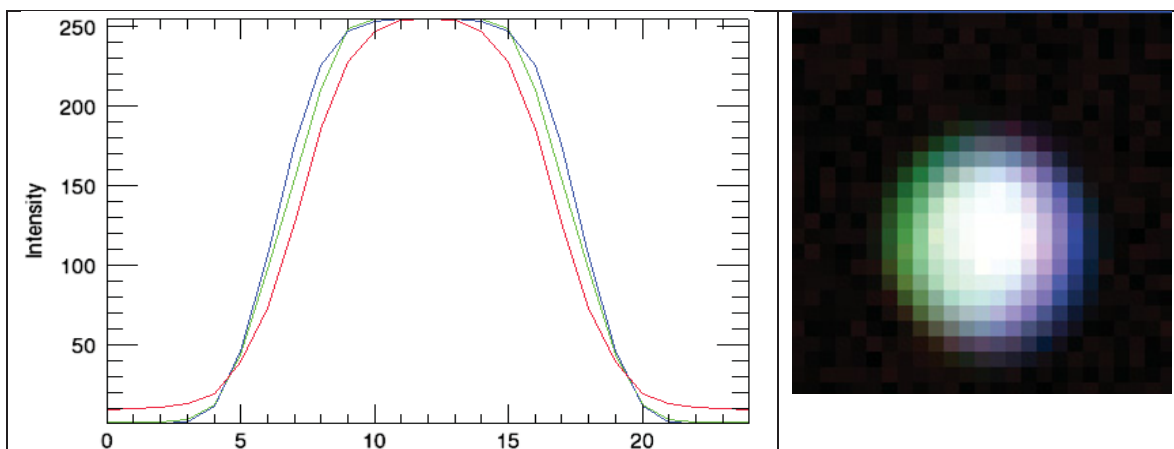


Table F4: Measurement of the FOV of the tilted 50 mm f/4 spherical mirror. Distance to object plane: $O+f=1500$ mm, focus offset adjustment: $df=40$ mm. (image plane)

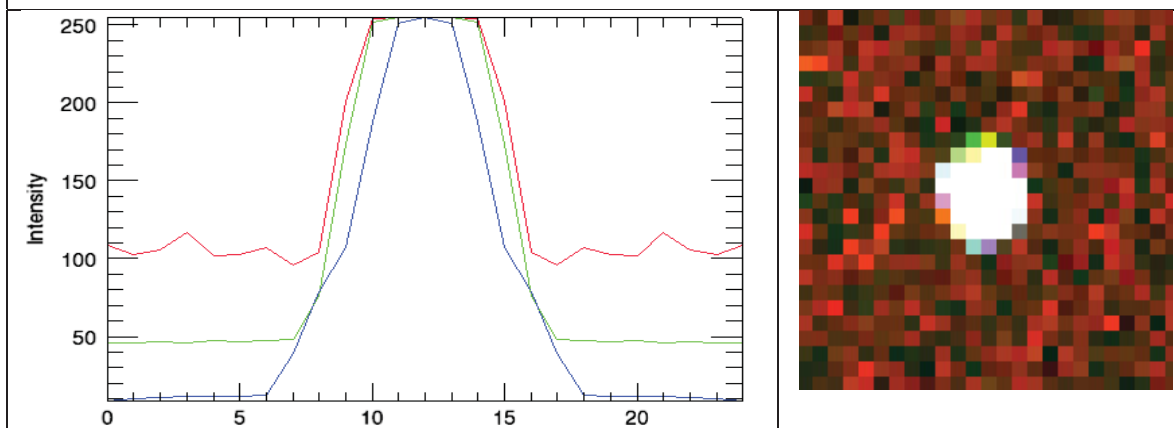


Table F5: Measurement of the FOV of the tilted 50 mm f/4 spherical mirror with. Distance to object plane: $O+f=1500$ mm, focus offset adjustment: $df=50$ mm.

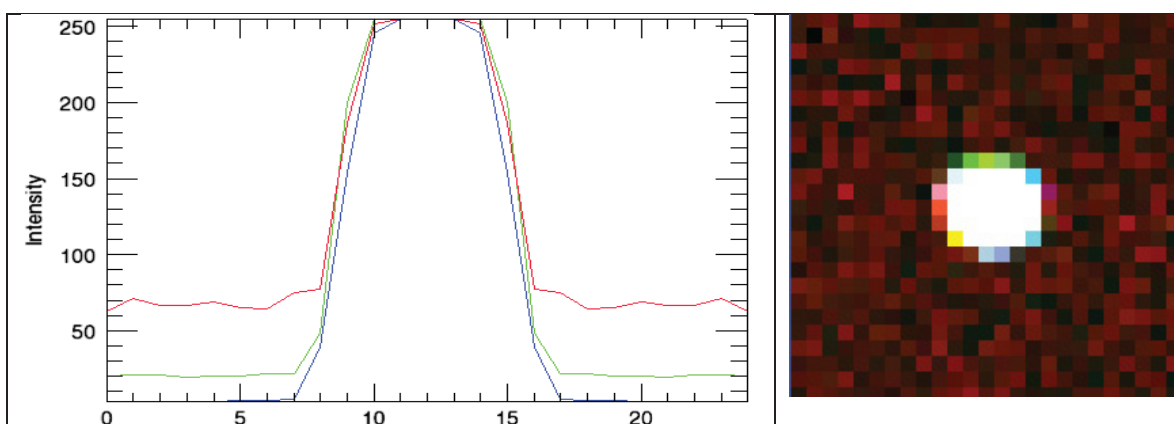
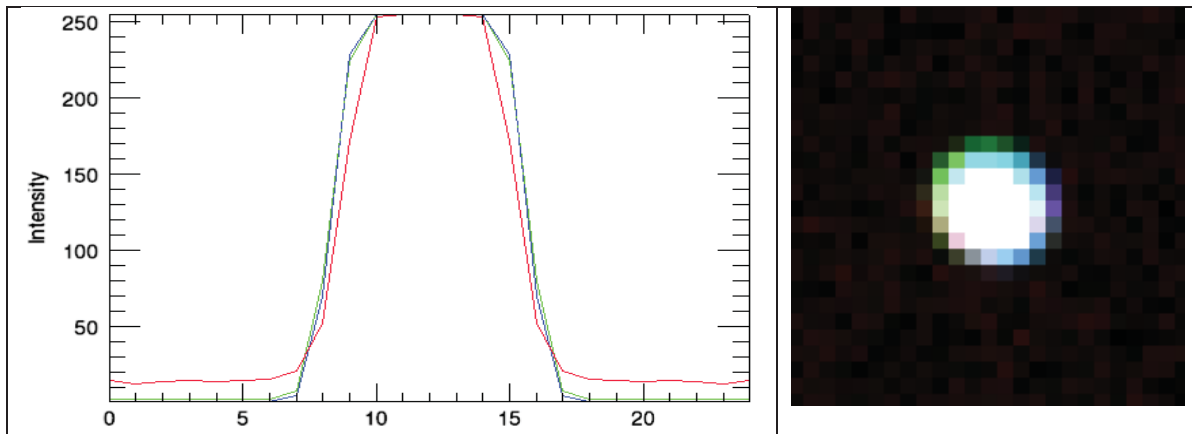


Table F6: Measurement of the FOV of the tilted 50 mm $f/4$ spherical mirror. Distance to object plane: $O+f=1500$ mm, focus offset adjustment: $df=60$ mm.



List of symbols/abbreviations/acronyms/initialisms

ASD	Analytical Spectral Devices
BRDF	Bidirectional Reflectance Distribution Function
DND	Department of National Defence
DRDC	Defence Research & Development Canada
DRDKIM	Director Research and Development Knowledge and Information Management
FOV	Field of View
R&D	Research & Development
df	Offset distance from the optical focal point (not from the image plane)
f/n	f/number: ratio focal length / optic diameter
f	Focal length
i	Distance of the image plane
O	Object distance

DOCUMENT CONTROL DATA		
(Security markings for the title, abstract and indexing annotation must be entered when the document is Classified or Designated)		
1. ORIGINATOR (The name and address of the organization preparing the document. Organizations for whom the document was prepared, e.g., Centre sponsoring a contractor's report, or tasking agency, are entered in Section 8.) Defence Research and Development Canada – Valcartier Research Center 2459 de la Bravoure Road Quebec (Quebec) G3J 1X5 Canada		2a. SECURITY MARKING (Overall security marking of the document including special supplemental markings if applicable.) UNCLASSIFIED
		2b. CONTROLLED GOODS (NON-CONTROLLED GOODS) DMC A REVIEW: GCEC DECEMBER 2012
3. TITLE (The complete document title as indicated on the title page. Its classification should be indicated by the appropriate abbreviation (S, C or U) in parentheses after the title.) Measurement of the spatial distribution of the spectral response variation in the field of view of the ASD spectrometer input optics		
4. AUTHORS (last name, followed by initials – ranks, titles, etc., not to be used) Levesque, M. P.; Giroux, S.; Ardouin J. P.		
5. DATE OF PUBLICATION (Month and year of publication of document.) December 2014	6a. NO. OF PAGES (Total containing information, including Annexes, Appendices, etc.) 67	6b. NO. OF REFS (Total cited in document.) 10
7. DESCRIPTIVE NOTES (The category of the document, e.g., technical report, technical note or memorandum. If appropriate, enter the type of report, e.g., interim, progress, summary, annual or final. Give the inclusive dates when a specific reporting period is covered.) Scientific Report		
8. SPONSORING ACTIVITY (The name of the department project office or laboratory sponsoring the research and development – include address.) Defence Research and Development Canada – Valcartier Research Center 2459 de la Bravoure Road Quebec (Quebec) G3J 1X5 Canada		
9a. PROJECT OR GRANT NO. (If appropriate, the applicable research and development project or grant number under which the document was written. Please specify whether project or grant.) 6CB07	9b. CONTRACT NO. (If appropriate, the applicable number under which the document was written.) 	
10a. ORIGINATOR'S DOCUMENT NUMBER (The official document number by which the document is identified by the originating activity. This number must be unique to this document.) DRDC-RDDC-2014-R122	10b. OTHER DOCUMENT NO(s). (Any other numbers which may be assigned this document either by the originator or by the sponsor.) 	
11. DOCUMENT AVAILABILITY (Any limitations on further dissemination of the document, other than those imposed by security classification.) Unlimited		
12. DOCUMENT ANNOUNCEMENT (Any limitation to the bibliographic announcement of this document. This will normally correspond to the Document Availability (11). However, where further distribution (beyond the audience specified in (11) is possible, a wider announcement audience may be selected.) Unlimited		

13. **ABSTRACT** (A brief and factual summary of the document. It may also appear elsewhere in the body of the document itself. It is highly desirable that the abstract of classified documents be unclassified. Each paragraph of the abstract shall begin with an indication of the security classification of the information in the paragraph (unless the document itself is unclassified) represented as (S), (C), (R), or (U). It is not necessary to include here abstracts in both official languages unless the text is bilingual.)

A new goniometer is under development. It will be used for the measurement of the spectro-polarimetric BRDF (Bidirectional Reflectance Distribution function). For practical reasons, the selected spectrometer is an ASD field spectro-radiometer. Its optical head is built with an optical fibre cable bundle that makes it easy to use. Only the optical head has to be mounted on the goniometer, the main body of the spectrometer remains aside. The ASD spectrometer has several input optics (bare fibres, lenses and telescopes) and several tests were conducted to determine which one is the best for the goniometer. The conclusion: none of them. By construction, the ASD spectrometer does not have a homogeneous field of view (FOV). The optical fibre bundle does not uniformly sample the FOV. This can be partly solved by defocusing the optics. But, all the tested optics suffers from severe spectral dispersion or other artefacts. However, a simple optical design based on the use of an off-axis mirror can do the job. This will be used for the optical reading head of the goniometer.

Un nouveau goniomètre est en développement. Il sera utilisé pour les mesures de BRDF (fonction de distribution de réflectance bidirectionnelle) spectrales et polarimétriques. Pour des raisons pratiques, le spectromètre sélectionné est le spectro-radiomètre portable de la compagnie ASD. Sa tête optique est faite avec un câble de fibres optiques qui la rend facile à utiliser. Seulement la tête optique doit être montée sur le goniomètre, le corps principal du spectromètre reste à côté. Le spectromètre ASD a plusieurs optiques d'entrées (fibres nues, lentilles et télescopes) et plusieurs tests ont été faits pour déterminer lequel est le meilleur pour le goniomètre. La conclusion : aucun d'entre eux. De par sa construction, le spectromètre ASD n'a pas un champ de vue homogène. Le faisceau de fibres optiques n'échantillonne pas uniformément le champ de vue. Ceci peut être résolu en mettant l'optique hors foyer. Mais, toutes les optiques testées souffrent de dispersion spectrale sévère et de d'autres artefacts. Cependant, un design optique simple basé sur l'utilisation d'un miroir hors-axe peut faire l'affaire. Celui-ci sera utilisé pour faire la tête de lecture du goniomètre.

14. **KEYWORDS, DESCRIPTORS or IDENTIFIERS** (Technically meaningful terms or short phrases that characterize a document and could be helpful in cataloguing the document. They should be selected so that no security classification is required. Identifiers, such as equipment model designation, trade name, military project code name, geographic location may also be included. If possible keywords should be selected from a published thesaurus, e.g., Thesaurus of Engineering and Scientific Terms (TEST) and that thesaurus identified. If it is not possible to select indexing terms which are Unclassified, the classification of each should be indicated as with the title.)

Spectrometer, FOV. Field of view, spectral response, goniometer